AD NUMBER

AD871959

LIMITATION CHANGES

TO:

Approved for public release; distribution is unlimited.

FROM:

Distribution authorized to U.S. Gov't. agencies and their contractors; Critical Technology; 1970. Other requests shall be referred to Air Force Technical Applications Center, Alexandria, VA 22313. This document contains export-controlled technical data.

AUTHORITY

USAF ltr, 25 Jan 1972

TR 70-12

20

TECHNICAL REPORT NO. 70-12

LONG-PERIOD SEISMIC NOISE AND ATMOSPHERIC PRESSURE VARIATIONS

TELEDYNE GEOTECH

TECHNICAL REPORT NO. 70-12

LONG-PERIOD SEISMIC NOISE AND ATMOSPHERIC PRESSURE VARIATIONS

by

G. G. Sorrells
and
Zoltan Der

Sponsored by

Advanced Research Projects Agency
Nuclear Test Detection Office
ARPA Order No. 624

Availability

Qualified users may request copies of this document from:

Defense Documentation Center
Cameron Station
Alexandria, Virginia 22314

Acknowledgement

This research was supported by the Advanced Research Projects Agency, Nuclear Test Detection Office, under the technical direction of the Air Force Technical Applications Center under Contract No. F33657-69-C-0757.

NOTICE

THIS DOCUMENT IS SUBJECT TO SPECIAL EXPORT CONTROLS AND EACH TRANSMITTAL TO FOREIGN GOVERNMENTS OR FOREIGN NATIONALS MAY BE MADE ONLY WITH PRIOR APPROVAL OF CHIEF, AFTAC.

Alexandria, Va. 22313

TELEDYNE GEOTECH
3401 Shiloh Road
Garland, Texas

IDENTIFICATION

AFTAC Project No:	VT/8703
Project Title:	Long-Range Seismic Measurements
ARPA Order No:	624
ARPA Code No:	8F10
Contractor:	Geotech, A Teledyne Company
Date of Contract:	1 January 1969
Amount of Contract:	$1,185,191
Amendment 002:	$236,064
Contract No:	F33657-69-C-0757
Contract Expiration Date:	31 December 1969
Program Manager:	R. G. Reakes, 271-2561, Garland, Texas

CONTENTS

ILLUSTRATIONS

ILLUSTRATIONS, Continued

ABSTRACT

Preliminary studies of the long-period seismic noise and the atmospheric pressure fields were made at the Kleer mine near Grand Saline, Texas, during the winter of 1968. The results of the studies indicate that during periods of atmospheric turbulence the vertical and horizontal components of the seismic noise field observed at the surface may increase in total power by as much as 16 and 34 dB within the period range from 20 to 60 seconds. In contrast, long-period systems operated in the mine show little change in power levels regardless of the atmospheric conditions at the surface. The observations are consistent with the hypothesis that the increase observed at the surface is caused by atmospherically-generated deformations of the earth. However, because of questions regarding the surface vaults capability to attenuate pressure changes, the possibility that the noise was caused by vault leakage must be considered an equally likely explanation at the present time. The results indicate that atmospherically-generated seismic noise can seriously degrade the capability of a long-period surface installation to detect surface waves. Because of this finding, further more definitive studies are recommended.

PREFACE

The AR method and its derivatives provide a reliable discriminator between seismic signals generated by large magnitude underground nuclear explosions and earthquakes. Unfortunately, the technique cannot be applied to lower magnitude events because of a relatively high surface wave detection threshold. Since the identification of small magnitude events is of particular importance to undergound nuclear test detection, there is obviously a need to develop techniques to reduce the surface wave detection threshold or equivalently to attenuate the long-period seismic noise field. To date our studies have been devoted to an investigation of the relationship between long-period seismic noise and local variations in the atmospheric pressure field. The results of these studies are contained in this report.

This report is a compendium of three related studies. The first study describes the observations of the long-period seismic and atmospheric pressure fields made at the Kleer Salt Mine near Grand Saline, Texas. The basic result of this study is that the long-period noise power observed at the surface increases significantly during periods of atmospheric turbulence.

The second study is a preliminary theoretical investigation of one possible cause for the observed noise increase. In this paper, the response of an elastic half space to a plane pressure wave is evaluated in order to determine the conditions under which the pressure-generated displacements and tilts can contribute significantly to the seismic background. The basic result of this study is that at periods greater than 20 seconds and, in media with moderately low rigidities, displacements and tilts associated with pressure waves with amplitudes on the order of 100 microbars can contribute significantly to the seismic background. The results further indicated that if the speed of the pressure wave was small compared to the speed of the seismic waves in the medium the deformation could be described by the mathematics of static rather than dynamic elasticity.

The third study is devoted to the development of the mathematics necessary to describe the static deformation of a layered half space caused by an arbitrarily distributed surface load.

It is to be emphasized that the results presented in this report are of a preliminary nature. Observations with more sophisticated systems are presently being made, and more definitive studies of the relationship between long-period seismic noise and local atmospheric pressure fluctuations are underway. The results of these studies will be published in a later report.

BLANK PAGE

LONG-PERIOD SEISMIC NOISE AND ATMOSPHERIC PRESSURE VARIATIONS

1. INTRODUCTION

Recent theoretical studies by Sorrells (1969) and Der (1969) have indicated that variations in the atmospheric pressure field as small as 50-100 microbars can generate significant seismic noise at periods greater than 20 seconds. Experimental observations by Capon (1969) at the Montana LASA tend to confirm the theoretical studies and imply that elastic distortions of the surface of the earth induced by variations in atmospheric pressure are indeed a major source of long-period seismic noise.

During the winter of 1968, a long-period micorbarograph and two long-period seismograph systems were operated at the Kleer Mine near Grand Saline, Texas. The records produced by these systems were examined in order to obtain more information regarding the possible relationship between long-period seismic noise and local fluctuations in the atmospheric pressure field. The purpose of this particular report is to document the results of the preliminary study, to evaluate their significance, and to outline plans for further study.

2. DATA COLLECTION

A three-component long-period seismograph system, a long-period microbarograph, and an anemometer were operated at the surface. In the mine, the basic sensor systems included not only a three-component long-period system, but a vertical and horizontal short-period system as well. Block diagrams of the surface and mine data sensing and recording systems are shown in figure 1. The system responses of the long-period seismic and microbarographic systems are shown in figures 2 and 3, respectively. The seismic sensors used at the surface were installed in typical portable system vaults, which consist of a hole approximately 2 feet deep, plywood-earth retaining walls set in approximately 4 inches of concrete. The space around the seismometer was filled with fiberglass batting. Then the vault was closed with a plywood cover, two layers of fiberglass batting, and a sheet of clear polyfilm. The seismometers used in the mine were set on the floor. Both the mine and surface long-period vertical seismometer cases were sealed while the horizontal seismometer cases were not. The vertical separation of the mine and surface systems was approximately 600 feet while as shown in figure 4 the horizontal separation was approximately 400 feet.

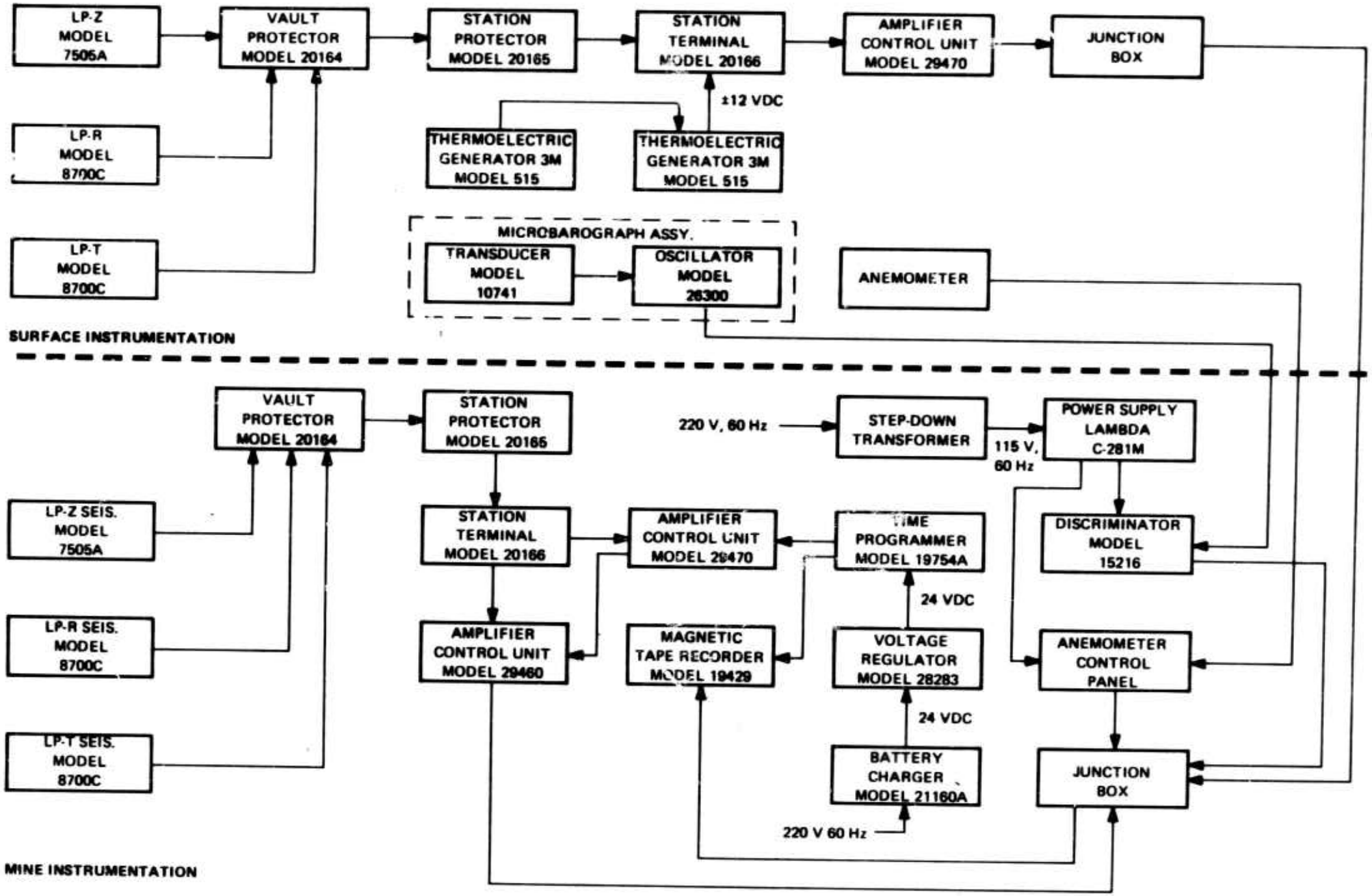

Figure 1. Block diagram of the instrumentation systems operated at Grand Saline, Texas

G 5811

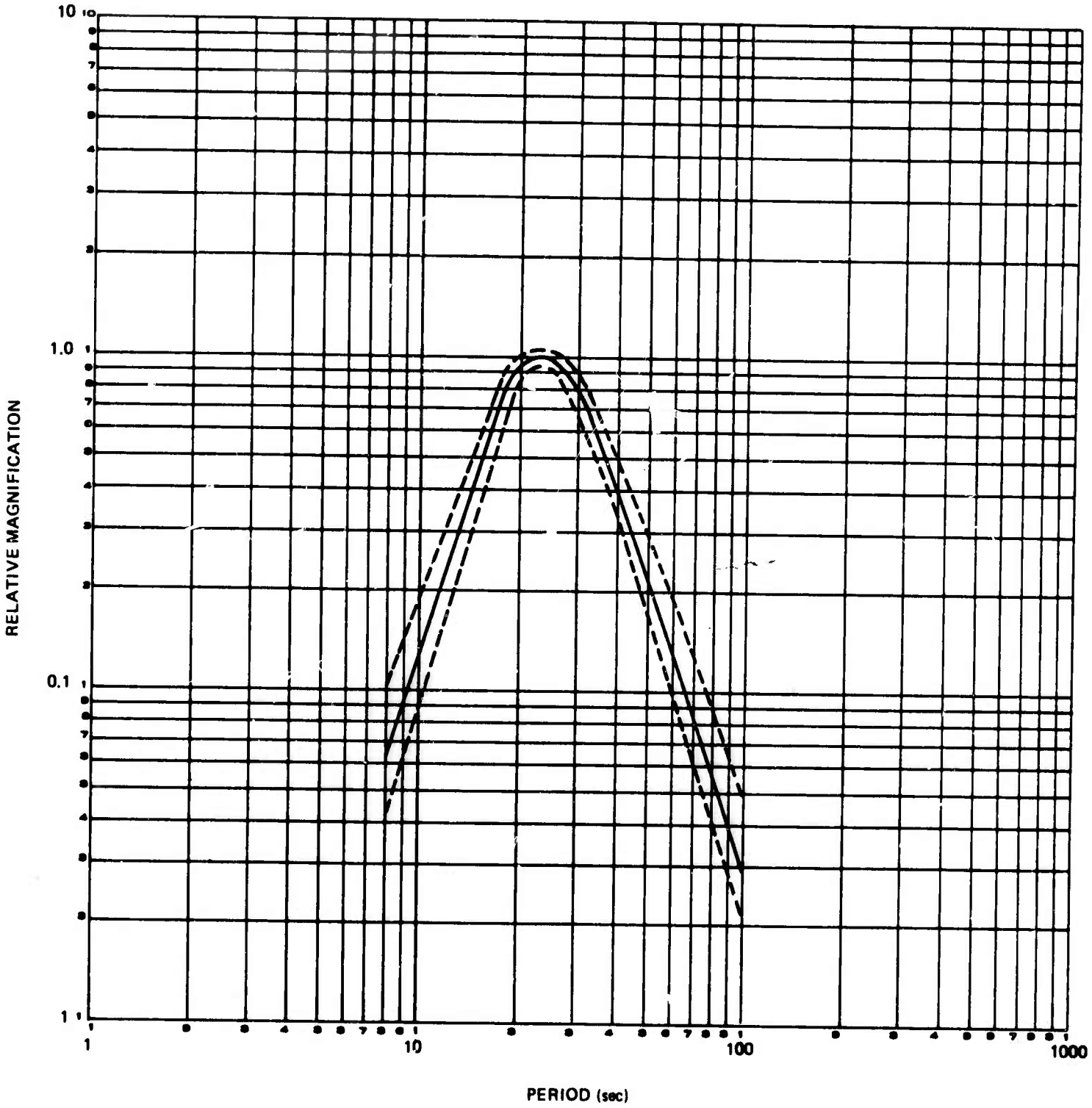

Figure 2. System response of the long-period seismographs operated at Grand Saline, Texas

G 5812

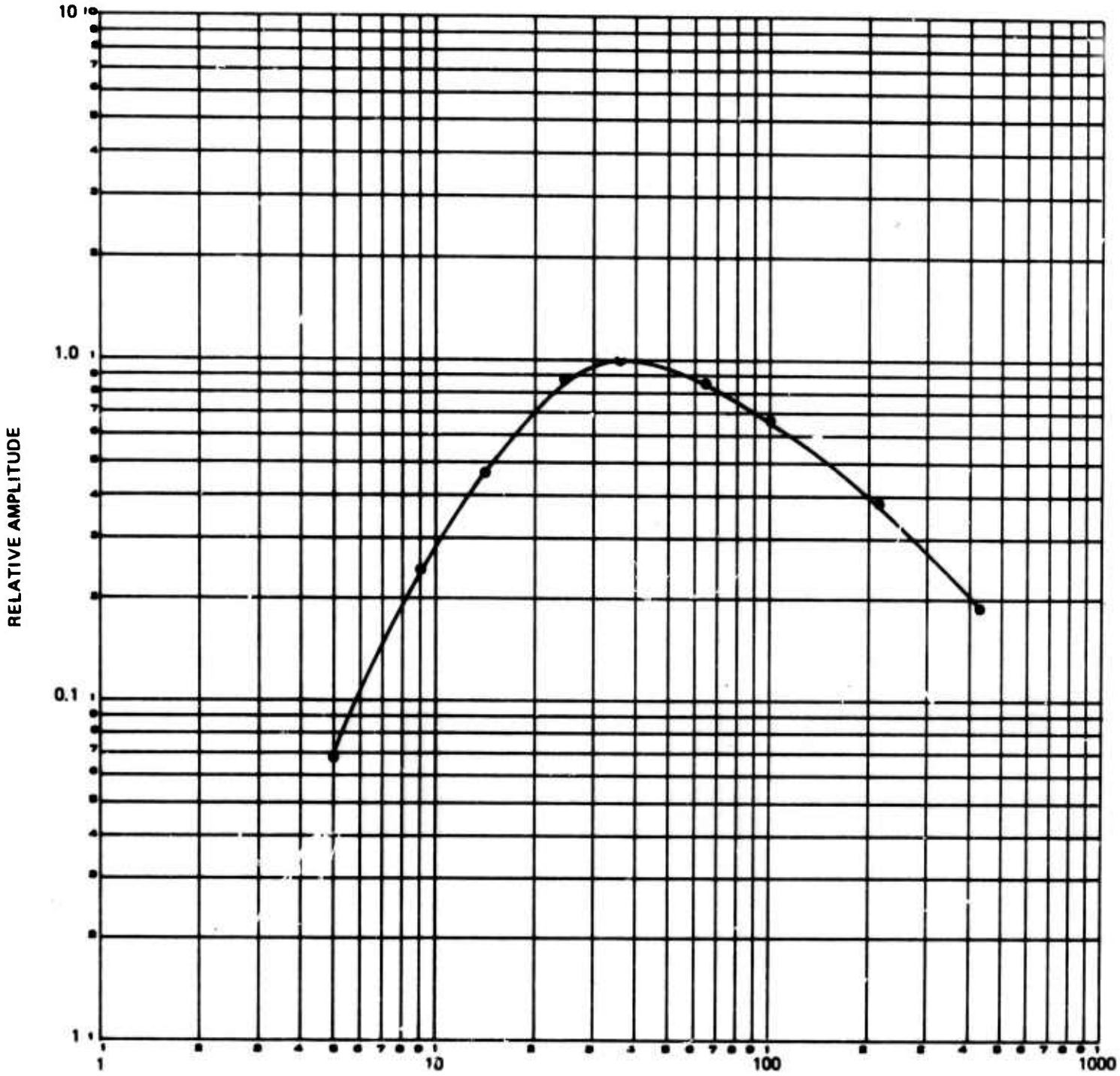

Figure 3. System response of the long-period microbarograph operated at Grand Saline, Texas

G 5813

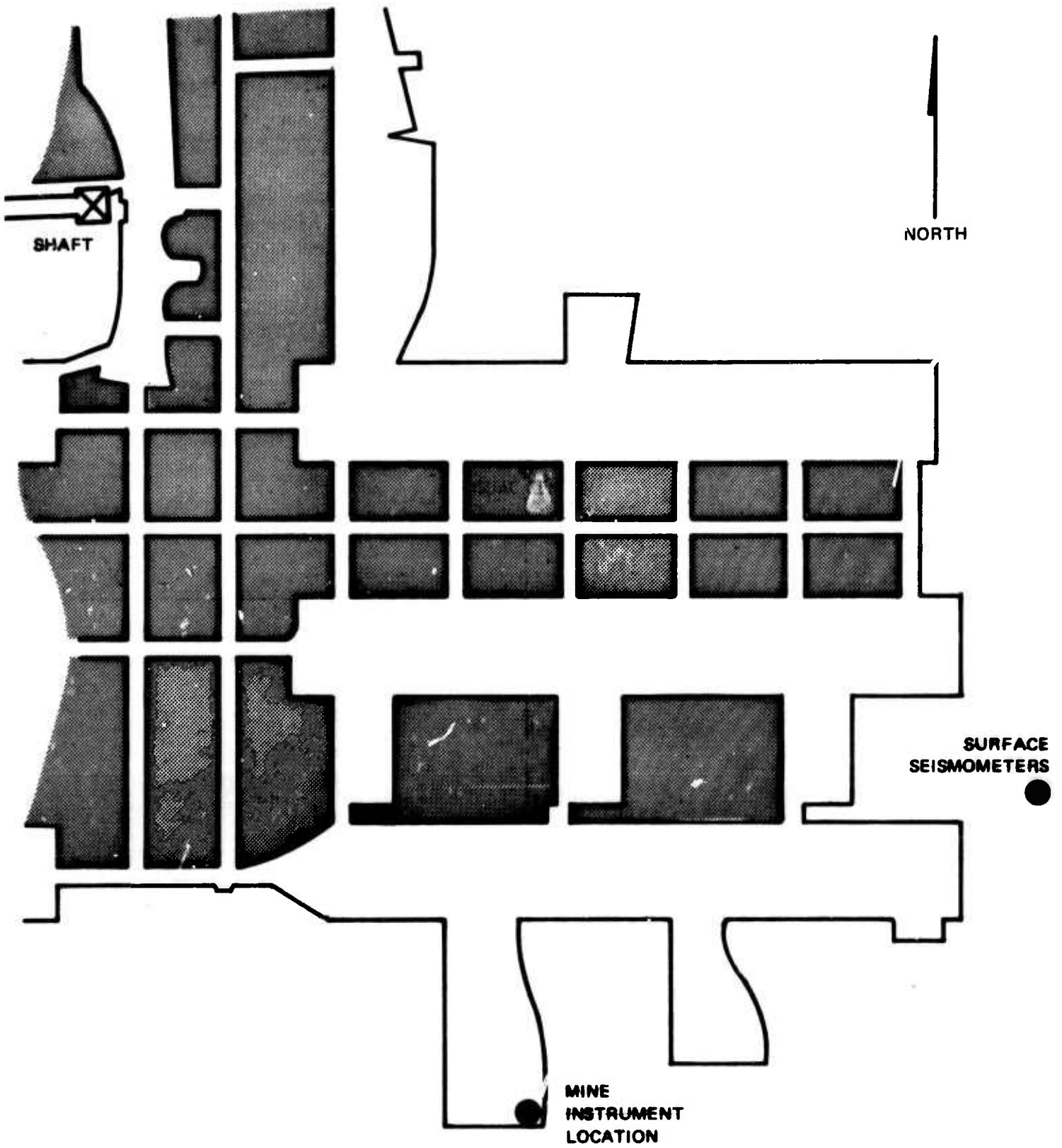

Figure 4. Sketch map of the Kleer mine showing the relative location of the mine and surface systems

G 5814

3. DATA ANALYSIS

Power density spectra for individual records and coherency spectra for selected pairs of records were the basic analytical tools used during this investigation. These were computed from record segments chosen to represent various conditions of atmospheric pressure variations. A total of six such segments, each approximately 30 minutes in duration, were selected for the preliminary analysis. The selection was made from 16-mm film reproduction of the data stored on magnetic tape. Within each of the selected time intervals, the outputs of both sets of seismographs and the microbarograph were low-pass filtered to prevent aliasing, digitized at the rate of two samples per second, then multiplexed and stored on digital tapes. Prior to computing the power and coherency spectra, the seismic data were normalized by dividing by the magnification at 25 seconds; and linear trends were removed from both the seismic and microbarographic records. Both the power density and cross power density spectra were computed from blocks of 3700 points using 127 lags and Parzen smoothing. Power density spectra were computed for all records. Cross power density, coherency and phase spectra were computed for corresponding seismic records taken on the surface and in the mine. In addition, cross power density, coherency, and phase spectra were computed for records taken from the microbarograph and the surface horizontal seismographs. Examples of the results of the computation are displayed and discussed in the next section.

4. DISCUSSION OF RESULTS

4.1 RECORDS TAKEN DURING CALM PERIODS

The power spectra shown in figure 5 are typical of the seismic data recorded on the vertical seismographs during calm periods. Note that for periods less than about 20 seconds, the spectral content of the noise observed on the surface and in the mine is virtually the same. This was not unexpected since the seismic noise in the period range from 6-20 seconds is known to consist primarily of fundamental mode Rayleigh waves with wavelengths much greater than the distance separating the two observation points. The coherency measurements shown in figure 6 confirm that within this period range the noise recorded by both systems is identical. At the longer periods, however, the situation is quite different. As seen in figure 6, there is a progressive reduction in the coherence between the noise observed on the surface and within the mine. This is accompanied by a monotonic increase in the noise power observed on the surface relative to that observed in the mine (see figure 7). Clearly, there is no apparent relationship between the seismic noise observed by the two systems within this period range.

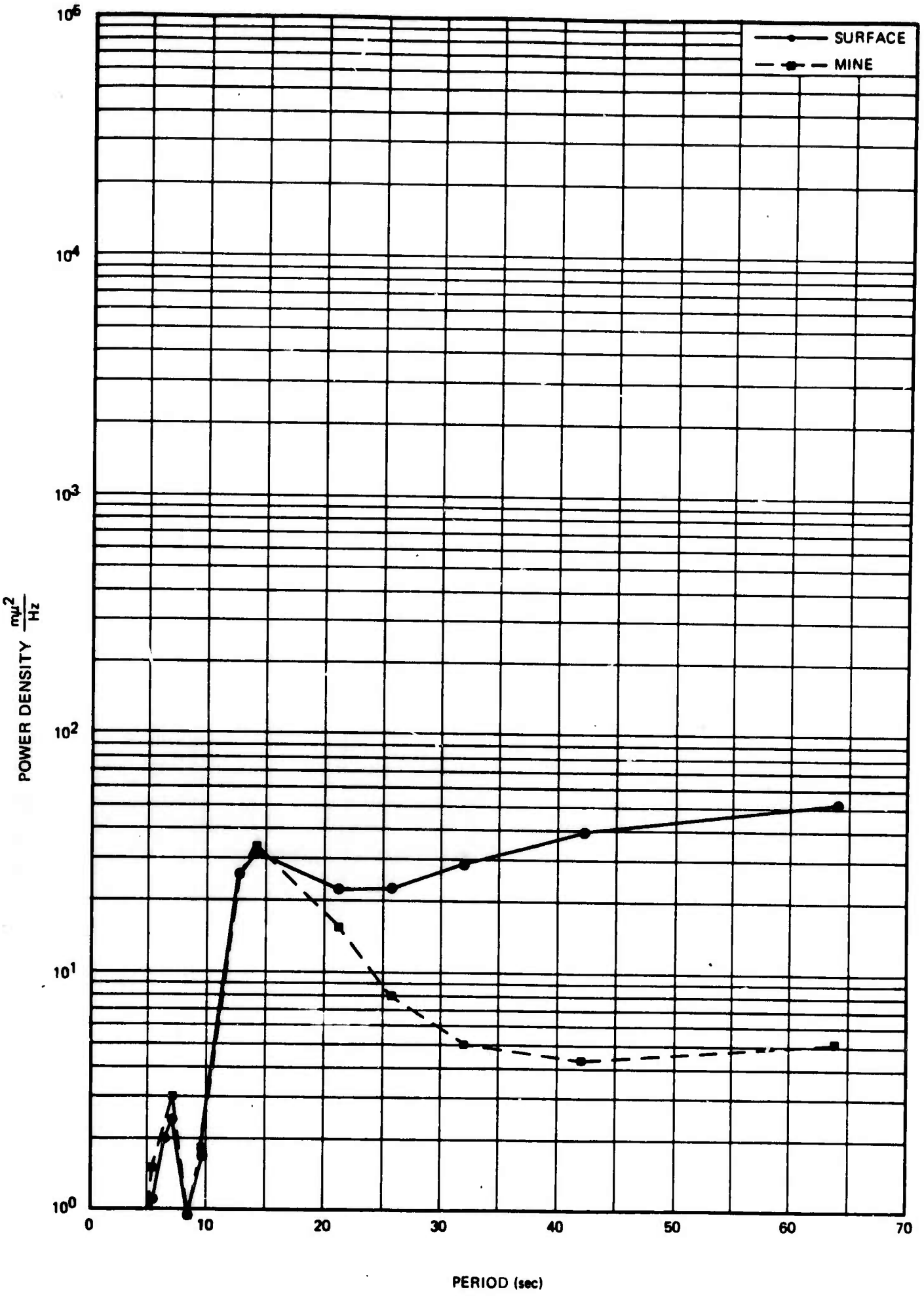

Figure 5. Power spectra typical of the data recorded in the mine and on the surface by the vertical seismographs during a calm period. Spectra are not corrected for instrument response.

G 5815

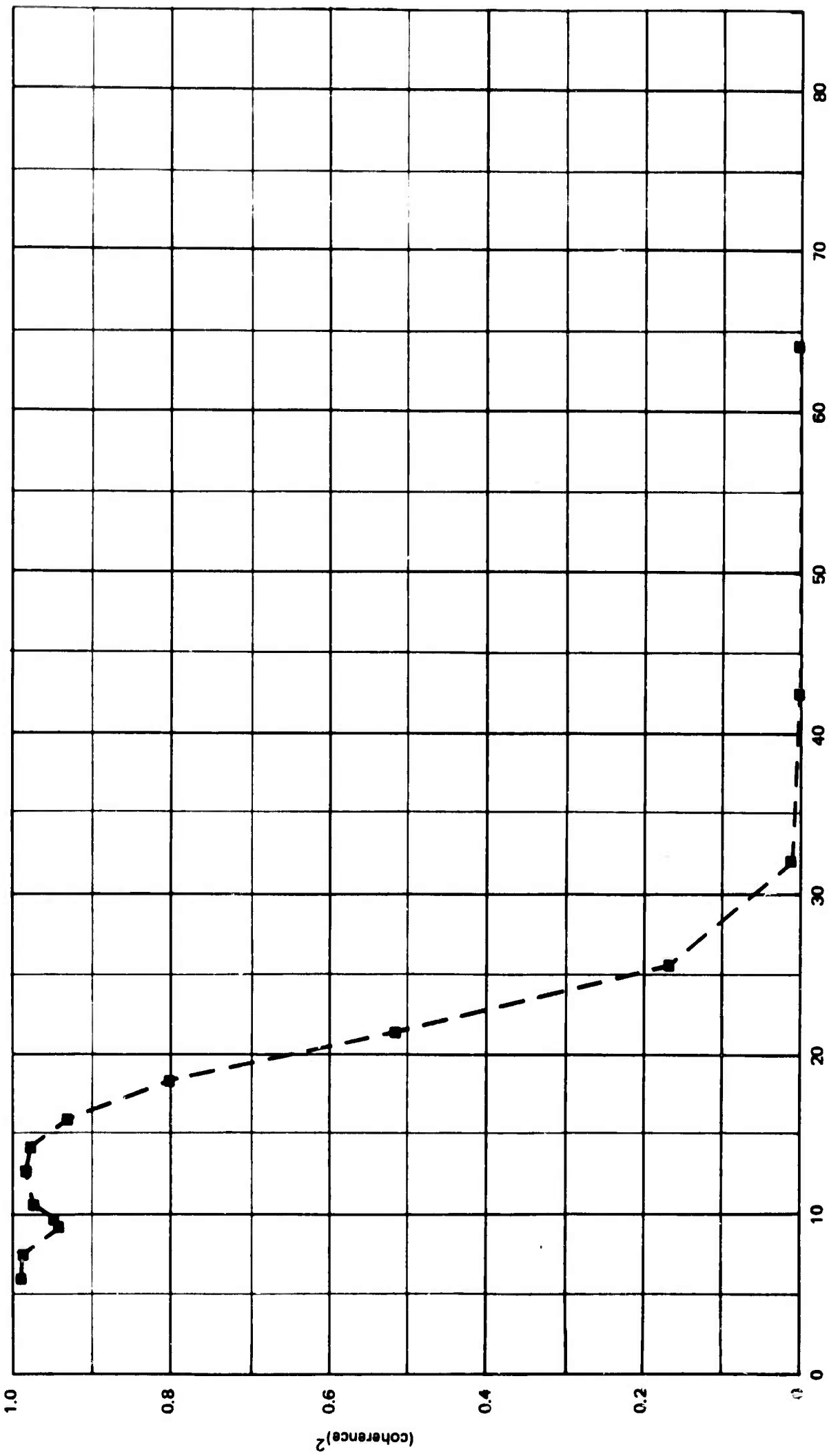

Figure 6. The coherence between data recorded by the mine and surface vertical seismograph during a calm period

G 5816

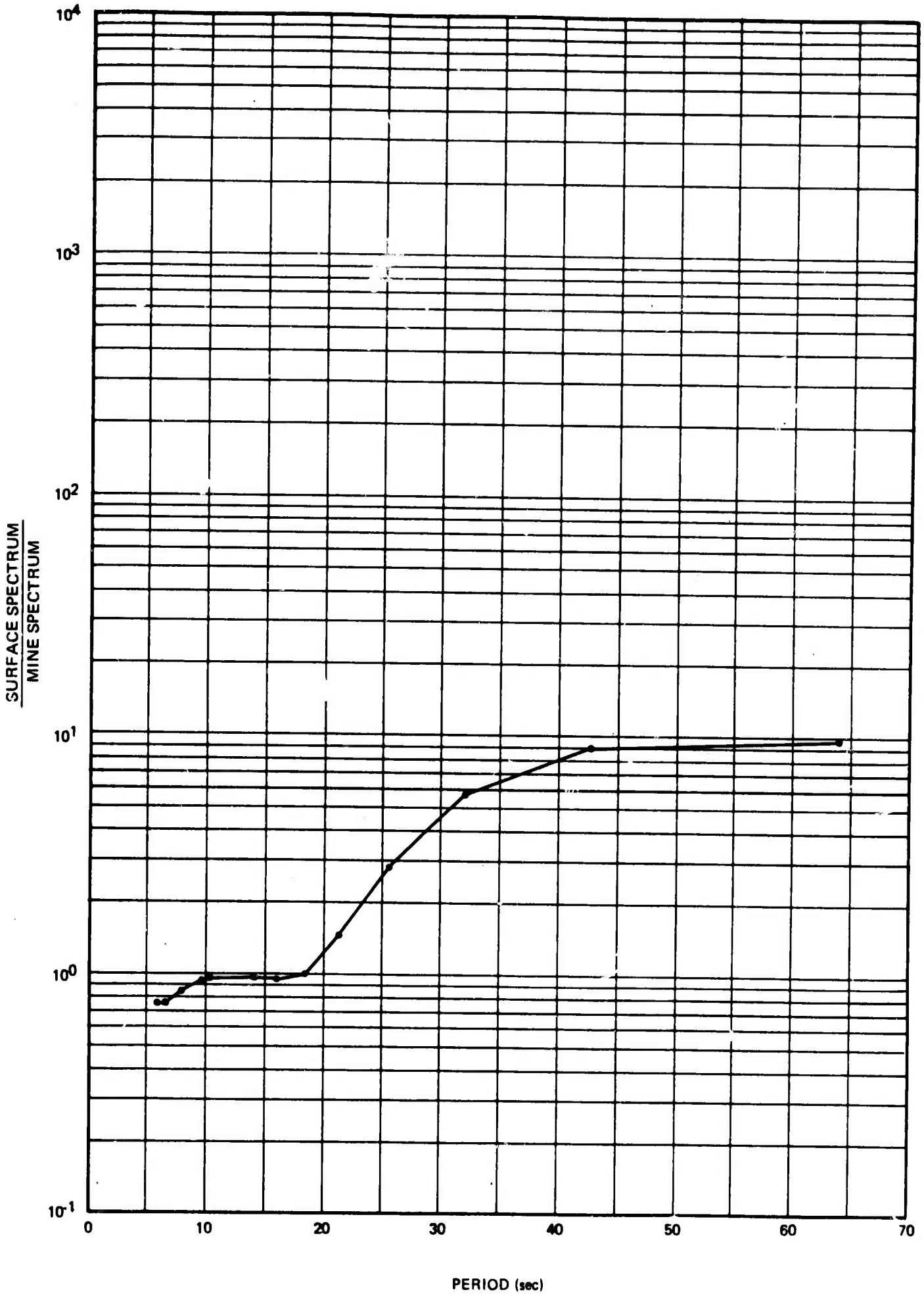

Figure 7. The ratio of the power spectrum observed on the surface relative to the power spectrum observed within the mine during a calm period

G 5817

The data recorded by the horizontal seismographs during calm periods show some characteristics similar to those described in the previous paragraph. An example of the power spectra computed from data taken from the transverse horizontal seismographs located on the surface and in the mine are shown in figure 8. These were computed from data taken during the same interval of time as the vertical data discussed previously. The coherence between the two sets of horizontal data is shown in figure 9. Like the vertical data the horizontal spectra may be divided into two period ranges; a short-period range characterized by high coherence in which the power levels observed upon the surface and within the mine are the same, and a long-period range within which the two data sets are incoherent and the noise power observed upon the surface is considerably higher than that observed in the mine. The principal difference is that, whereas, the 15-second microseism peak is clearly visible on both vertical spectra, it is almost completely obscured on the horizontal spectra. The interfering fields as recorded by the two horizontal seismographs are apparently generated by independent sources as shown by the reduction in the coherence of the 15-second peak. The fact that even during calm periods the noise at periods greater than about 15 to 20 seconds is considerably higher on the surface than in the mine merits further consideration. It cannot be related to variable atmospheric conditions because the samples analyzed were specifically selected from intervals of time during which there were no measureable wind and microbaric activity was minimal. This conclusion is further reinforced by the fact that there is no coherence between data recorded by the microbarograph and by the vertical and horizontal seismographs (see figure 10). There are several possible explanations for the existence of the high noise at the surface. First of all, the noise could be system generated. This seems unlikely since it is found at a relatively high level only on the surface systems. A more likely explanation is that it is in some way associated with the type of installations used on the surface. It will be recalled from section 2 that while the surface vaults were covered, no specific attempts were made to tightly seal them. Thus, it is possible that some of the noise observed at the longer periods could be related to disturbances within the vault. Another possibility is that the noise is related to local surface activity associated with the operation of the mine. No conscious effort was made during this particular investigation to select samples during periods when activity associated with the mine was likely to be low. Thus, it is possible that the samples could be contaminated to some degree by noise generated through local surface activity. This possibility will be thoroughly examined during a forthcoming investigation.

4.2 RECORDS TAKEN DURING TURBULENT PERIODS

The power spectra shown in figure 11 and figure 12 display features that are typical of the data recorded by the vertical and horizontal seismographs during turbulent periods. The basic difference between these spectra and those taken during calm periods is the relatively large increase in the noise power observed at the surface. The nature of this increase may be seen more clearly from figure 13. In this figure, the ratio between the spectra observed at the surface during a calm and turbulent interval has been plotted as a function of period in the range from 20 to 64 seconds. Note that both the surface vertical and transverse ratios show a trend similar to the microbarographic ratio. All ratios tend to decrease in a regular manner as a function of increasing period.

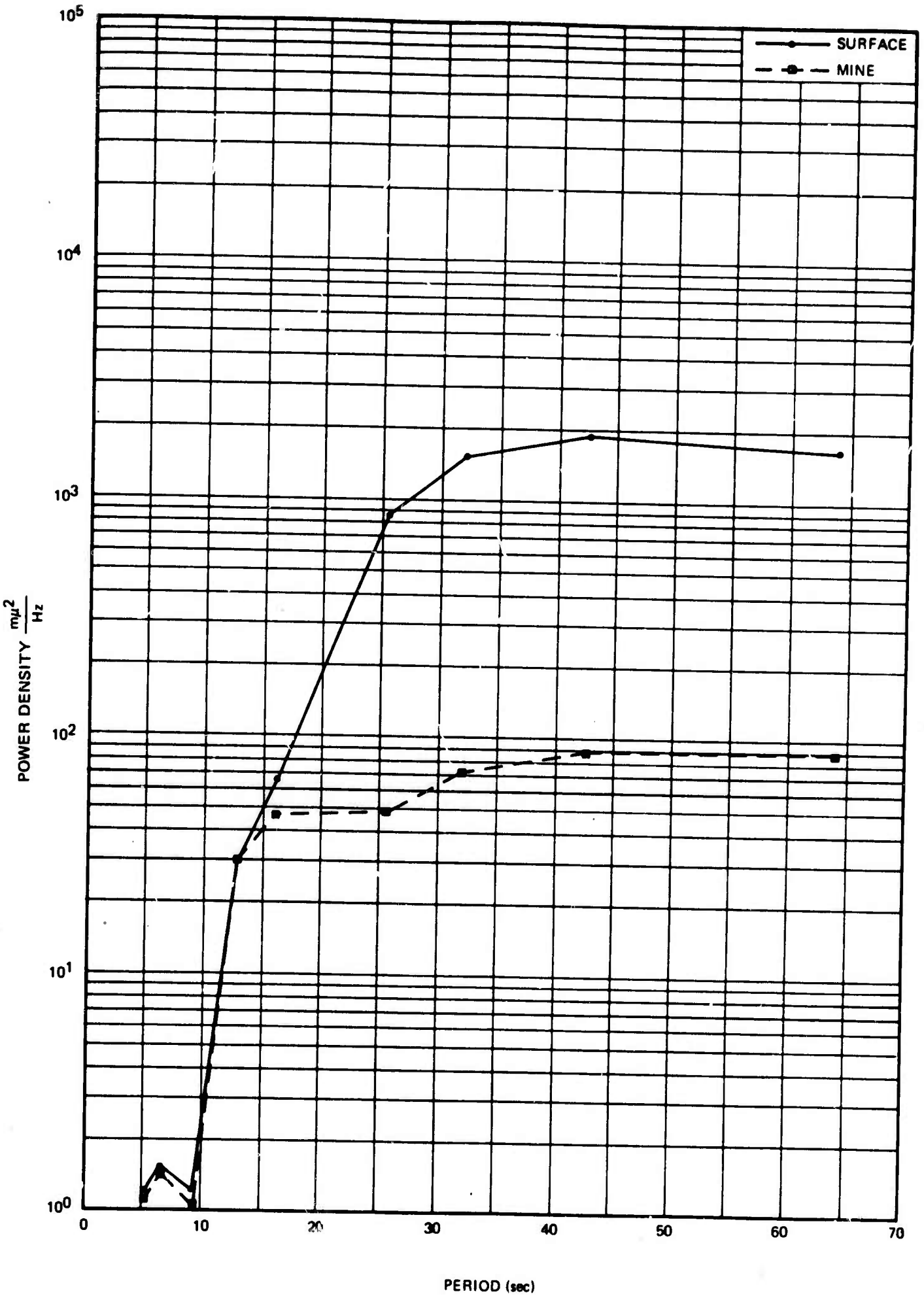

Figure 8. Power spectra typical of data recorded in the mine and on the surface by the transverse horizontal seismographs during a calm period. Spectra are not corrected for system response.

G 5818

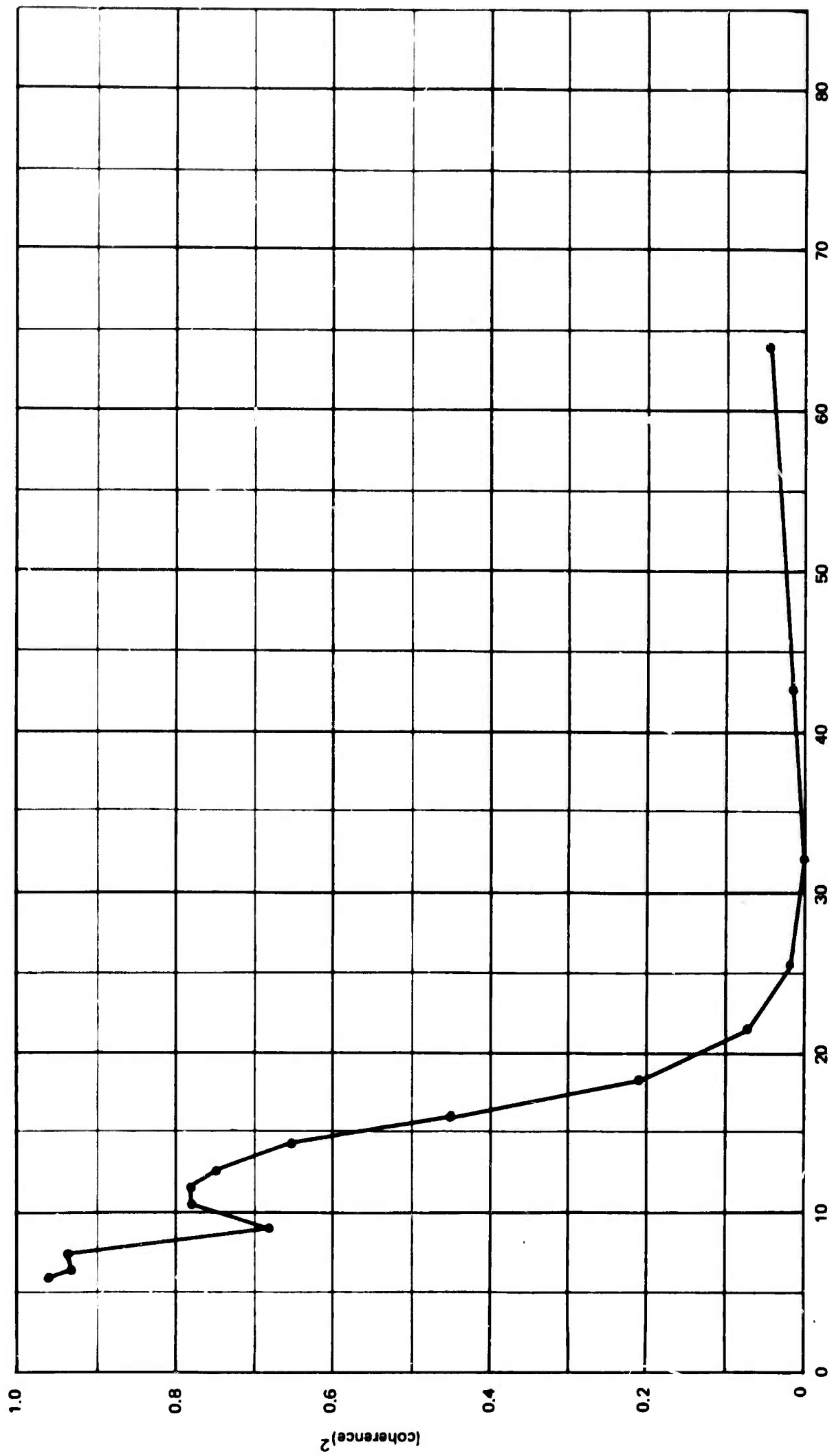

Figure 9. The coherence between data recorded by the transverse horizontal seismographs located in the mine and on the surface - data recorded during a calm period

G 5819

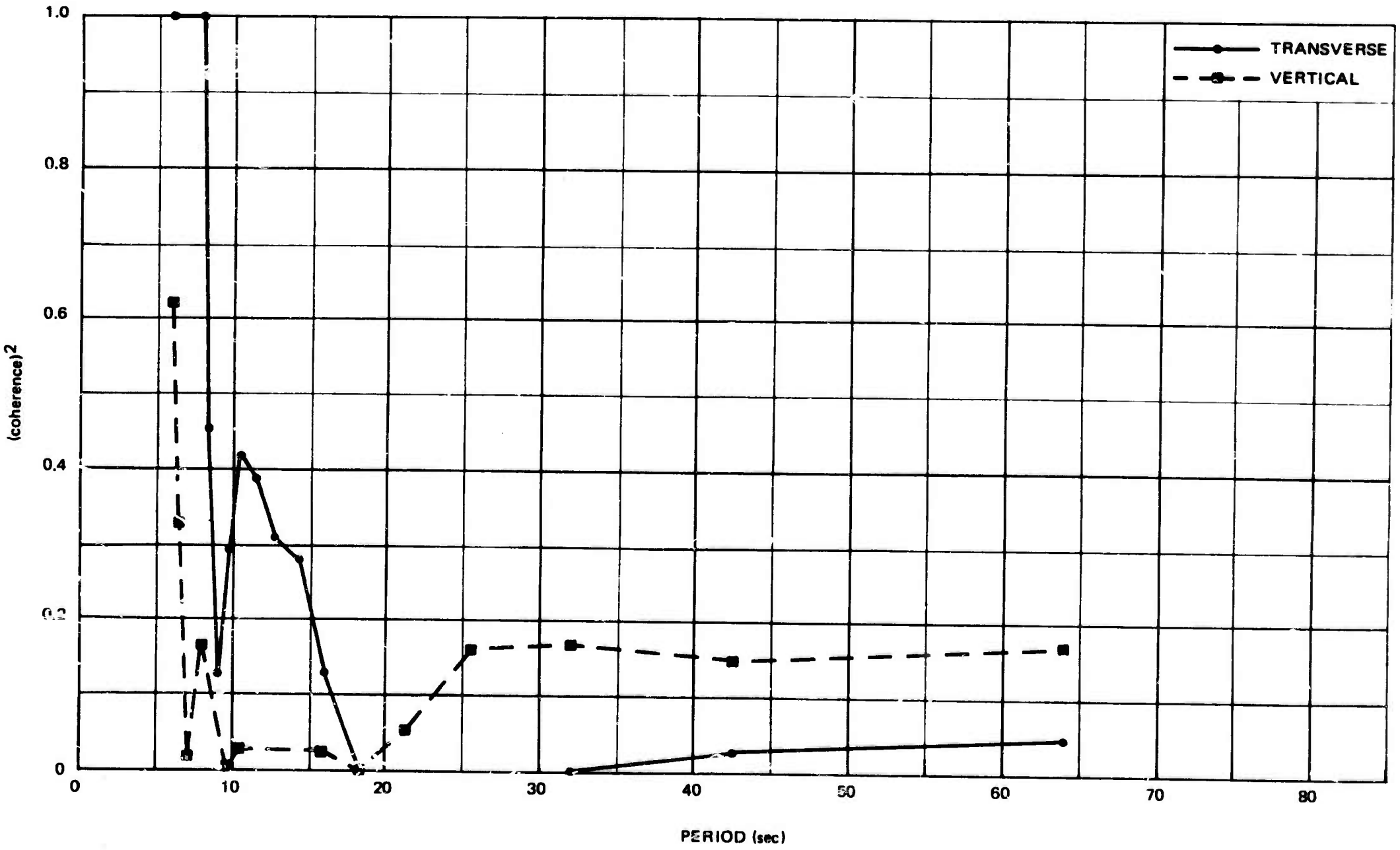

Figure 10. The coherence between the vertical and horizontal transverse seismographs located at the surface and the microbarograph - data recorded during a calm interval

G 5820

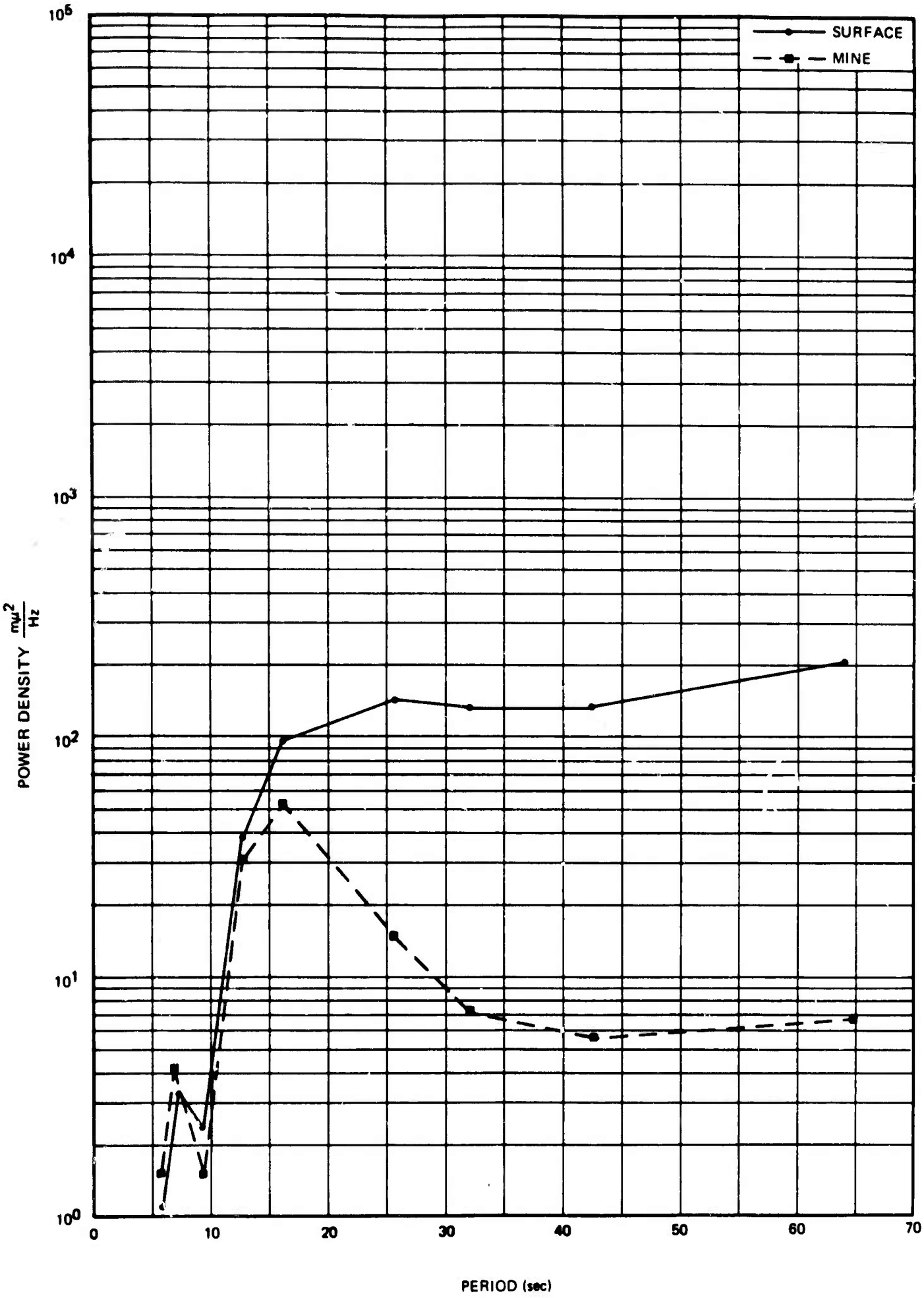

Figure 11. Power spectra computed from data taken from mine and surface vertical seismographs during a turbulent period. Spectra are not corrected for system response. G 5821

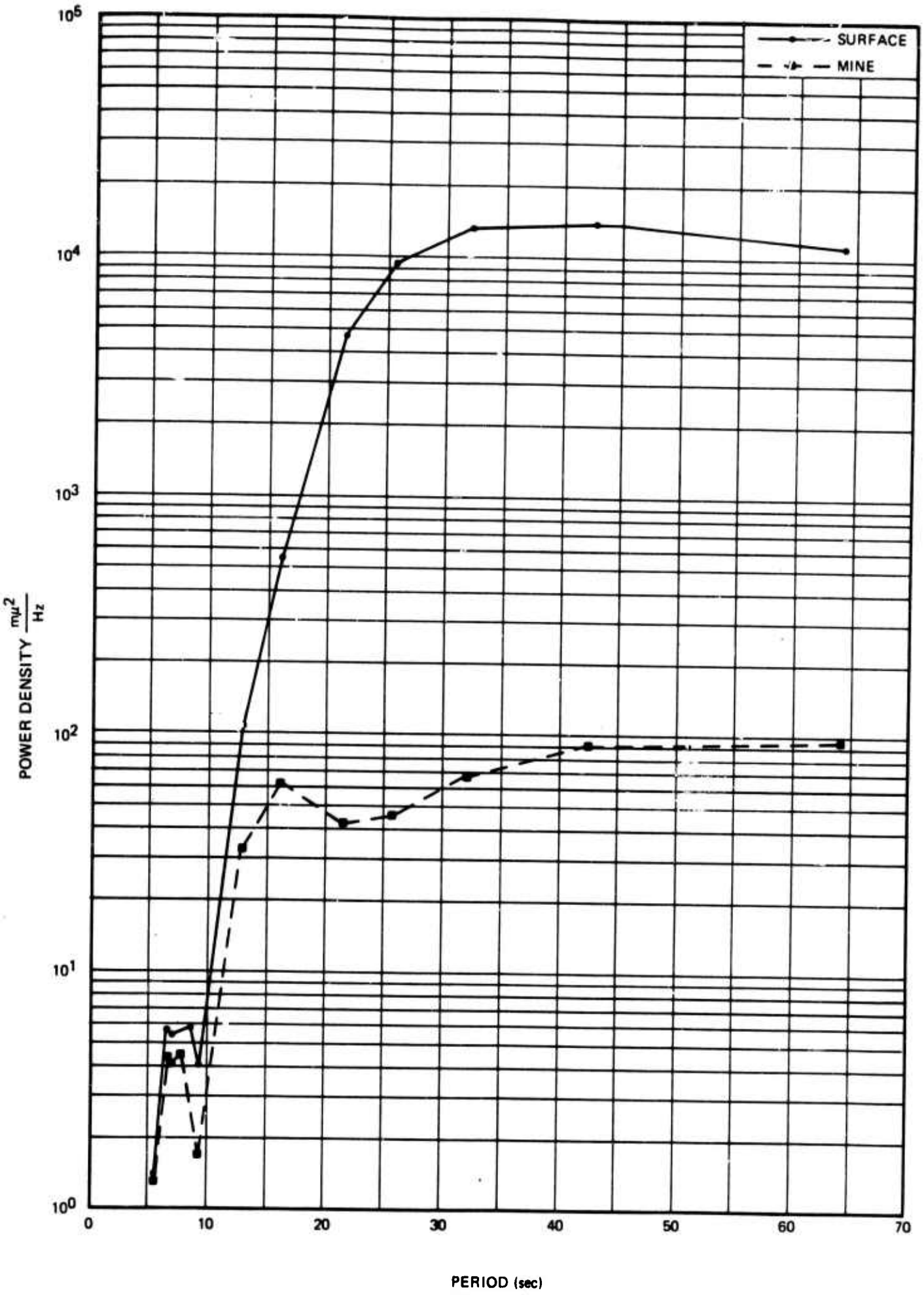

Figure 12. Power spectra computed from data taken from mine and surface horizontal transverse seismographs during a turbulent period. Spectra are not corrected for system response.

G 5822

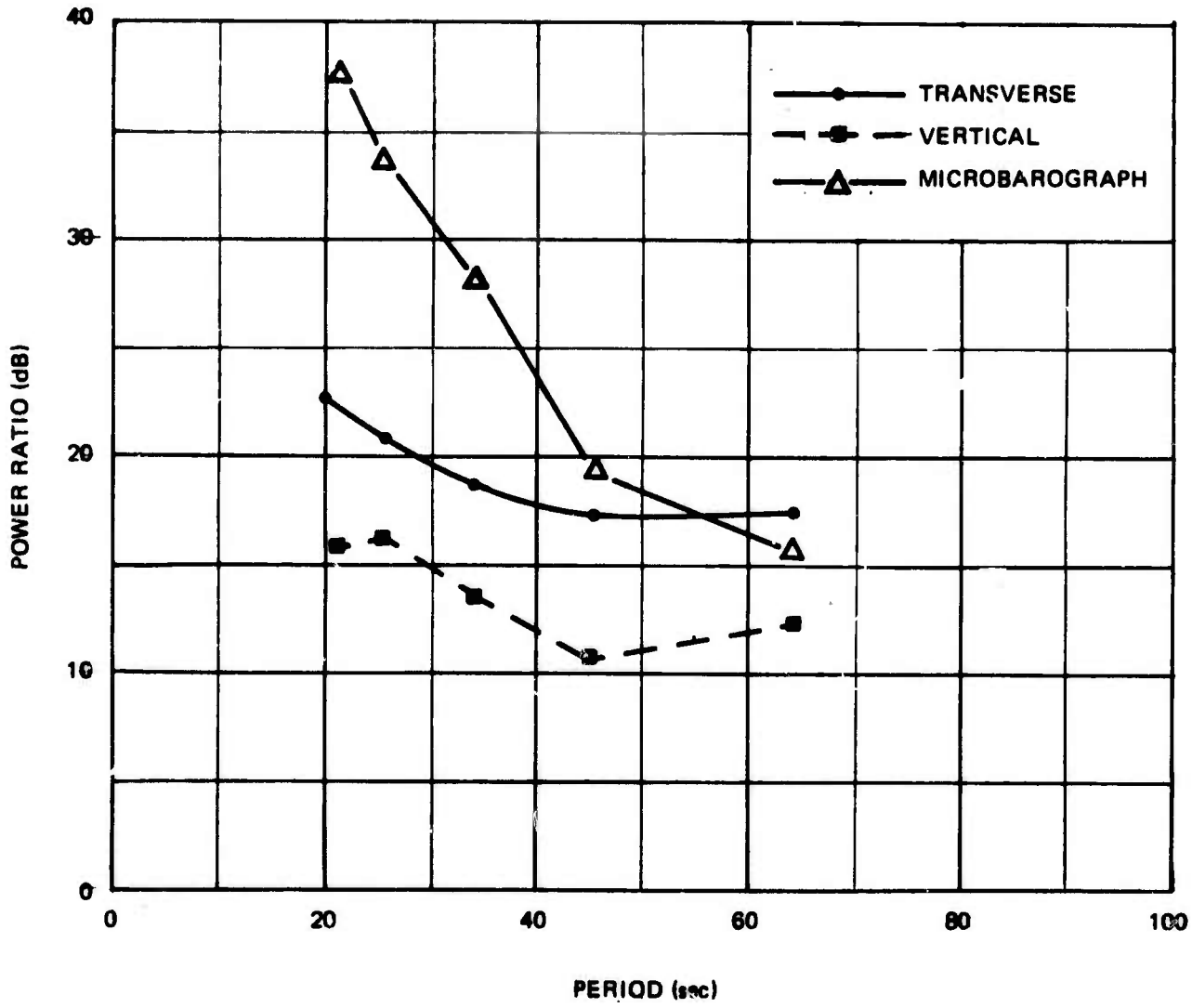

Figure 13. The ratio of the power spectra computed from data observed at the surface during a turbulent period relative to those computed from data recorded during a calm period

G 5823

However, both the values of the microbarographic ratios and their rate of decrease with increasing period is greater than for the seismic data. The results shown in this figure strongly suggest that the increase in the long-period noise field observed at the surface during turbulent intervals is directly related to increases in the atmospheric pressure field. Additional support for this contention comes from estimates of the degree of coherence between the data recorded by the microbarograph and the surface seismographs. These estimates are plotted as a function of increasing period in figure 14. Notice that at periods greater than about 20 seconds, a significant fraction of the total noise power observed by the transverse seismograph can be correlated atmospheric pressure variations. The degree of coherence between the microbarograph and the surface vertical is considerably smaller, indicating that the percentage of atmospherically-generated noise relative to the total field observed by this system is much lower than by that observed by the surface transverse. This is consistent with the observations given in figure 13, which show that the increase in the power of the vertical component of the noise field is about 6 dB less than the increase in the horizontal component.

In contrast to the seismic data observed at the surface, there is little significant change in the data recorded in the mine regardless of the atmospheric conditions. This may be seen from figure 15, in which the ratio of the power observed in the mine during calm and turbulent periods is plotted as a function of increasing period. The shaded area shown in this figure indicates the 90 percent confidence interval. Ratios which fall in this range cannot be considered significantly different from 1 (0 dB). Note that there is no significant difference in the power levels observed by the transverse horizontal seismographs in the period range from 20 to 64 seconds. The vertical component of the seismic noise field observed in the mine shows a small increase at periods less than about 30 seconds, but the increase is about 10 dB less than that observed at the surface. It is clear from these results that atmospheric turbulence at the surface does not contribute significantly to the seismic noise field in the mine.

In addition to the specific features described in the previous paragraphs, there is a general tendency for the seismic noise observed at the surface to increase as the noise recorded by the microbarograph increases. This tendency is illustrated in figures 16a and 16b. The diagrams were constructed in the following manner. First, both the seismic and the microbarographic spectra collected during various intervals of atmospheric turbulence were normalized to a common base by dividing them by the spectra collected during a calm period. Then, the normalized spectra were averaged over the period range extending from 21.3 to 64 seconds. The resulting number is a measure of the relative mean change in long-period power, which occurred during that interval as compared to the power observed during a calm interval. Then in order to delineate any possible relationship between changes in microbarographic power and changes in seismic power, the mean seismic values that were computed from data collected at the surface were plotted against the mean microbarographic power change characteristic of that interval. As shown in figures 16a and 16b, both the horizontal and vertical components of the surface seismic field tend to increase monotonically as the microbarographic power increases, but not at the same rate. The horizontal rate of increase appears to be considerably larger than the

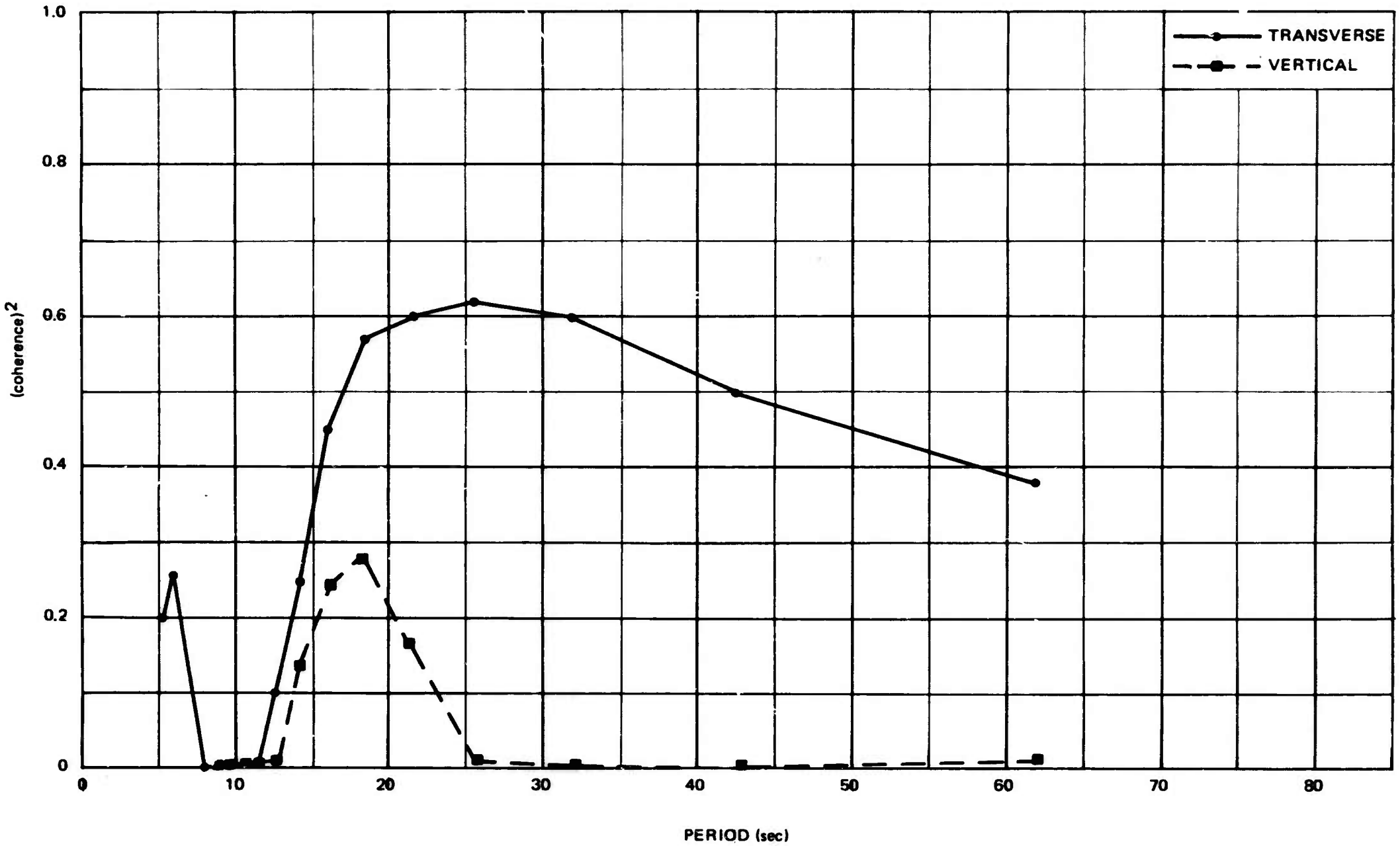

Figure 14. The coherence between the seismic data recorded at the surface and the microbarograph during a turbulent period

G 5824

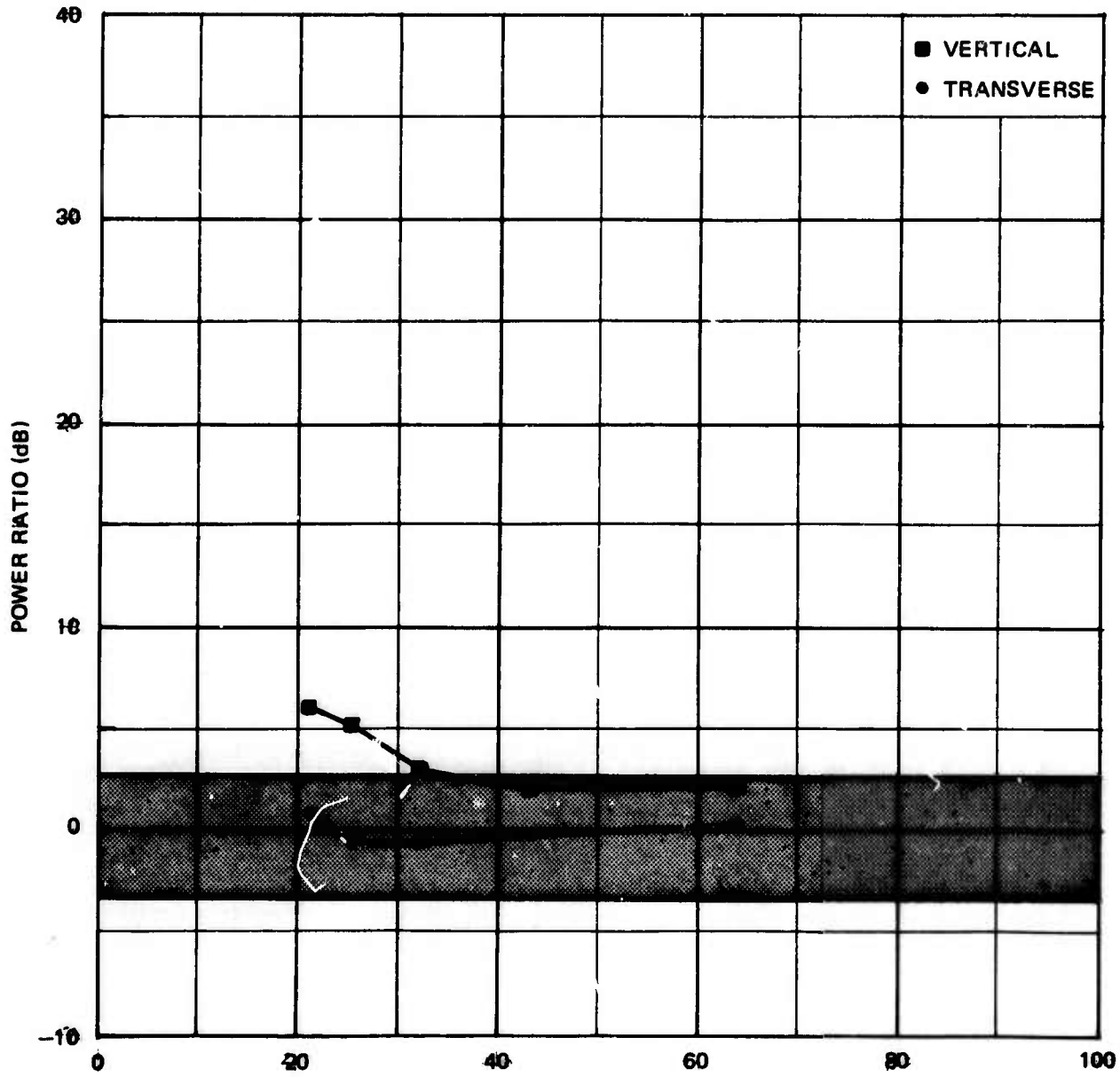

Figure 15. The ratio of the power spectra computed from data observed in the mine during a turbulent period relative to those computed from data recorded during a calm period

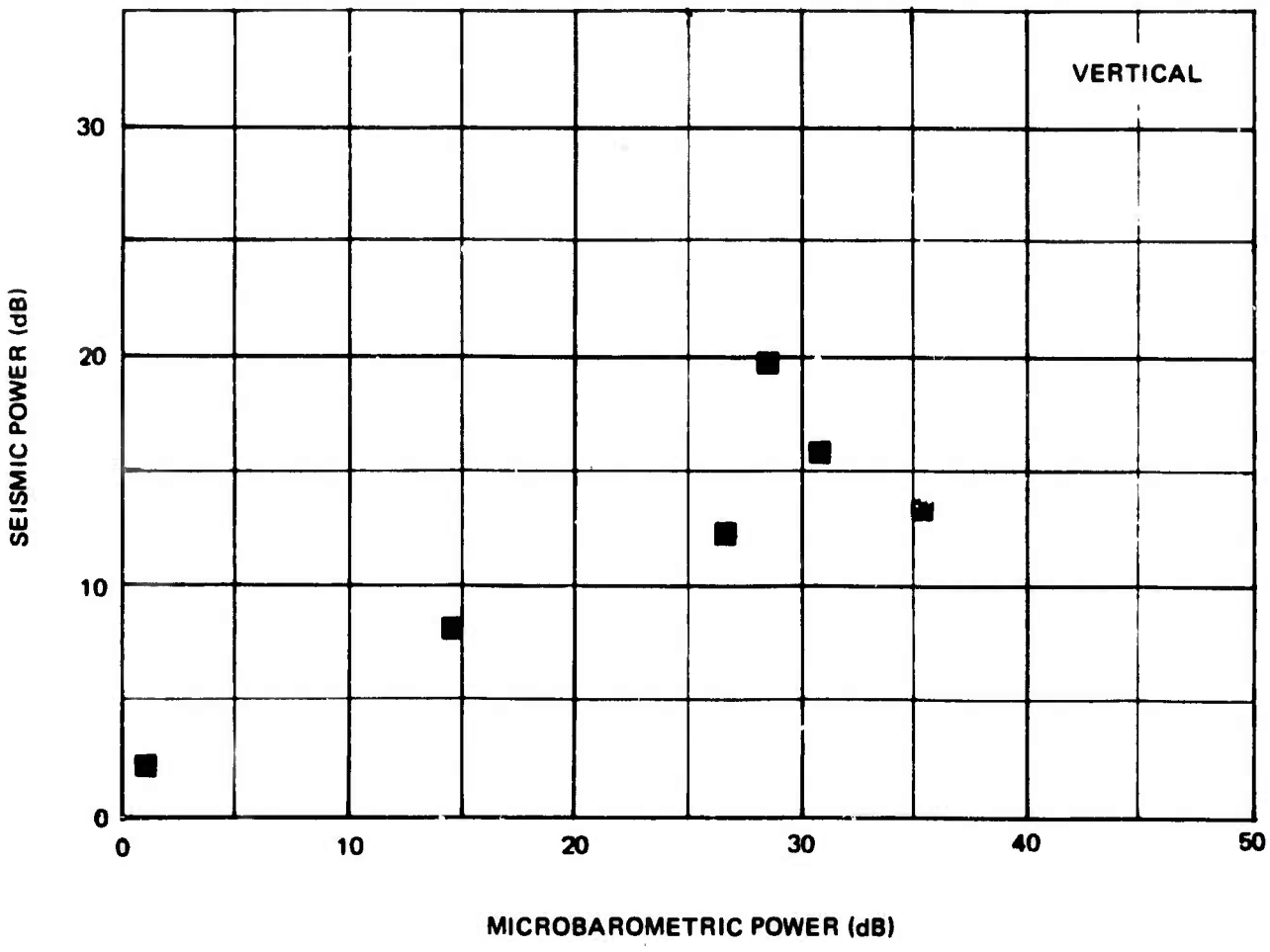

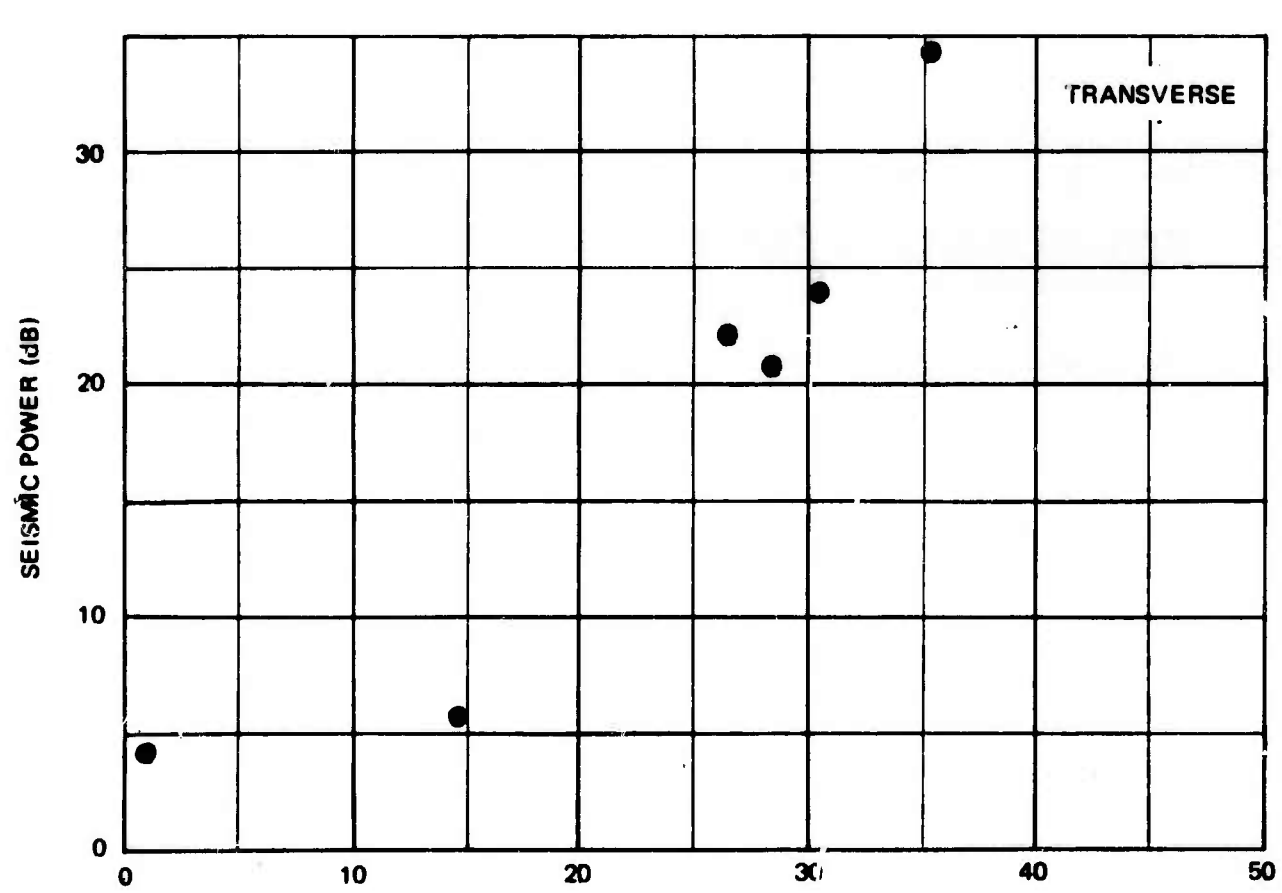

Figure 16. The mean increase in seismic noise power level observed at the surface versus the mean increase in the microbarographic noise power level G 5826

vertical. If similar seismic quantities computed from the data collected in the mine are plotted against relative increases in microbarographic power, the results shown in figures 17a and 17b are obtained. These data show that atmospheric pressure fluctuations at the surface have no apparent effect on the horizontal component of the long-period seismic noise field observed in the mine. The vertical component does show a weak tendency to increase as the microbarographic power increases; however, the rate of increase is much less than that observed on the surface.

5. SUMMARY OF RESULTS

The basic results of this preliminary investigation may be summarized in the following manner.

a. During calm intervals and in the period range from about 6 to 20 seconds, the power levels recorded in the mine and on the surface are quite similar and show a high degree of coherence indicating identical sources. At periods greater than 20 seconds, the coherence between the data recorded at the surface and within the mine decays rapidly and the power levels observed at the surface increase dramatically relative to those observed within the mine. The cause of the higher noise at the surface is not known at the present time.

b. During periods of atmospheric turbulence, the seismic noise field observed at the surface contains a component which is related to fluctuations in the atmospheric pressure. The addition of this component to the surface seismic field results in a general tendency for the total field to increase as the atmospheric pressure fluctuations intensify. This component appears to be absent or at least strongly attenuated in the seismic field observed in the mine.

6. EXPLANATION OF RESULTS

As stated previously, the cause of the relatively high noise levels observed at the surface during calm periods is not presently known. It could be caused by a variety of factors, none of which were specifically examined during the course of this investigation. Among these are the presence of higher system noise on the units operated at the surface; unspecified local noise associated with the nature of the surface installations; and noise created by activities associated with the operation of the mine.

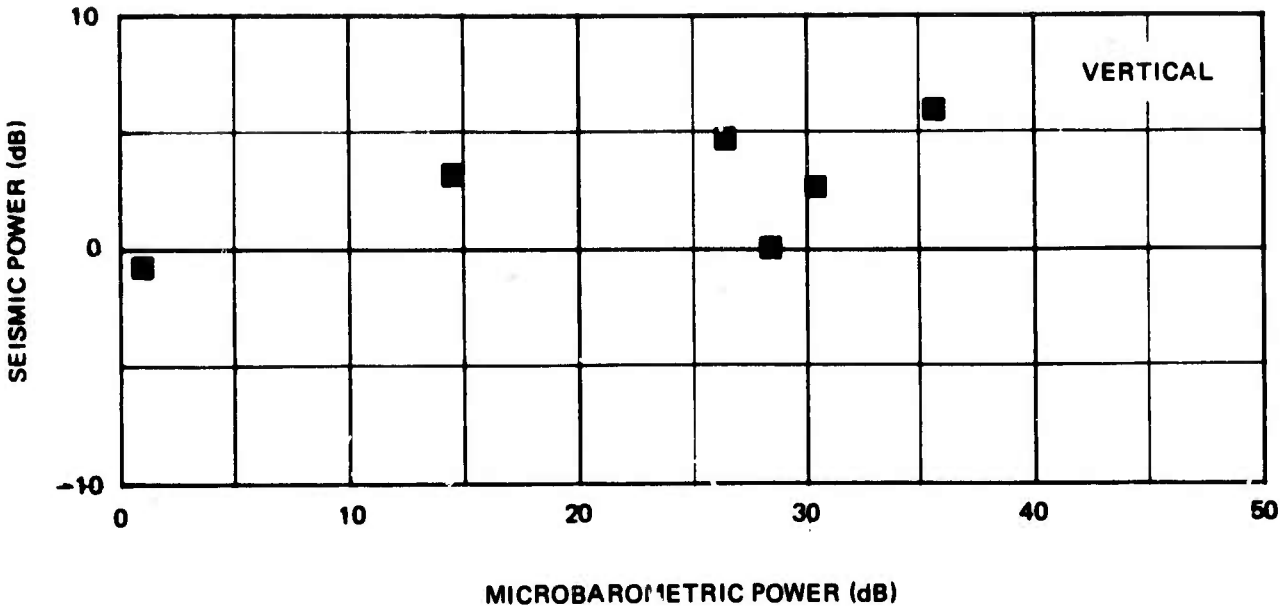

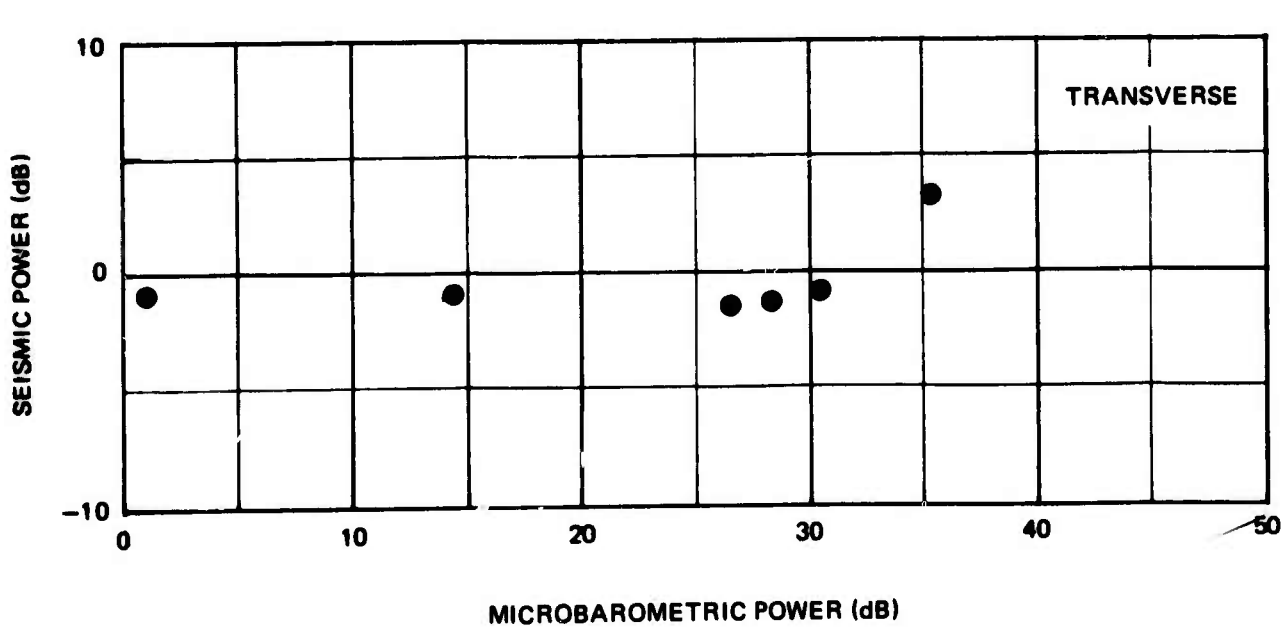

Figure 17. The mean increase in seismic noise power level observed in the mine versus the mean increase in the microbarographic noise power level

G 3827

The results presented display several attributes which suggest that during turbulent periods a significant fraction of the surface noise field could be related to elastic distortions of the surface caused by atmospheric pressure variations. The strongest arguments in favor of this interpretation are:

a. There is a significant reduction in the atmospherically-generated component of the long-period seismic noise field observed in the mine. This is in qualitative agreement with earlier calculations by Sorrells (1969), which indicated that if the noise were caused by variable atmospheric loads imposed upon the surface then at the depth at which the seismic systems were located (approximately 600 feet below the surface) it should be reduced by roughly 40 dB relative to its strength at the surface. Consequently, the general lack of an atmospherically-related component is consistent with the hypothesis of elastic loading by atmospheric pressure.

b. Durings periods of increased atmospheric noise power, the noise observed by the horizontal system increases more than the noise observed by the vertical system. This observation agrees qualitatively with Sorrells' results, which indicate that at periods greater than about 20 seconds a given pressure change will generate apparent horizontal displacements due to tilt, which are at least an order of magnitude greater than the corresponding vertical displacements. Thus, if the increase in the seismic noise field observed at the surface were caused by pressure-generated distortions of the surface, then the increase in noise power should be much greater on the outputs of the horizontal systems than on the vertical.

It must be stressed that these observations do not prove the hypothesis that the noise increase observed during turbulent intervals is caused by pressure-generated distortions of the earth. They merely argue for its plausibility. Until steps can be taken to assure that the surface vaults do not pass atmospheric pressure variations in the period range from about 20-60 seconds, the possibility that the noise increase is caused by pressure variations within the vaults must be considered an equally likely explanation.

7. SIGNIFICANCE OF RESULTS

The observations reported have a direct bearing on the problem of detecting long-period surface waves. It has been shown that during intervals of moderate atmospheric turbulence and within the period range from 20-60 seconds the vertical component of the surface seismic noise field can increase by as much as 16 dB in power, while the horizontal component can increase by as much as 34 dB in power. These numbers imply that a station's capability to detect surface waves can be seriously degraded during periods of atmospheric turbulence. This phenomena is by no means isolated to the Grand Saline area. Capon (1969) has shown that at the Montana LASA and within the period range 20-40 seconds atmospherically-generated noise makes up at least 40 percent of the total power at least 50 percent of the time.

It also has been shown that the noise levels observed within the mine stay essentially the same regardless of the atmospheric conditions at the surface. This phenomena is apparently related to the fact that the seismic disturbances created by variable atmospheric loading dissipate very rapidly with depth as predicted by Sorrells (1969). Van Saggern (1970) has reported similar observations at Murphy Dome, Alaska, so that the absence of atmospherically-generated seismic noise at moderate depths is not unique to Grand Saline.

These observations when taken together imply that the surface wave detection capability of a given site or array of sites can be significantly improved by locating the sensors at moderate depths. This improvement would be the result of two factors. First of all, the observations documented in this report indicate that the vertical component of the noise field would be reduced by as much as 6-8 dB in amplitude and the horizontal components would be reduced by as much as 17 dB in amplitude. Secondly, after removal of the atmospherically-generated fraction, the remainder of the noise field, at least in the period range from 20-40 seconds, is anticipated to be coherent over relatively large distances (Capon, 1969). Thus, arrays and multichannel filtering techniques could be employed to achieve a further reduction of about 6 dB. Therefore, the total increase in surface wave signal-to-noise ratio could be as much as 12-14 dB. If such a gain could be realized it would raise the surface wave detection capability to a level comparable to the present short-period P wave detection capability.

One further point should be made. Recently there has been considerable interest in altering the response of long-period systems so that reliable observations of seismic data with periods up to 100 seconds can be made. The observations reported in the previous paragraphs are pertinent to this problem in that they indicate that a significant fraction of the noise in the period range extending from 20 seconds is related to atmospheric turbulence. It is anticipated that this noise will become even more intense as the period range is extended. The reasons for this are as follows:

a. It has been generally observed that the atmospheric pressure increases linearly with increasing period.

b. The earth's vertical displacement response to atmospheric pressure variations also increases linearly with the period (Sorrells, 1969).

c. The horizontal seismometer's tilt response increases as the square of the period (Rodgers, 1968).

Since significant atmospherically-related seismic noise has already been observed at the shorter periods, it can be concluded from the statements listed above that it will constitute an even greater fraction of the noise observed at the longer period ranges. Thus, it appears likely that in order to achieve high magnifications with the extended range long-period systems they must be operated at depths on the order of 200 to 300 meters or greater.

8. RECOMMENDATIONS

In view of the significance of these preliminary observations to the problems of surface wave detection, it is recommended that the studies be continued at Grand Saline. The basic objectives of these studies will be:

a. To determine the source of the relatively high noise levels observed at the surface during calm periods and, if possible, eliminate;

b. To estimate the fraction of seismic noise power, within a pass band extending from about 30 to 100 seconds, which can be attributed directly to atmospherically-generated deformations of the earth.

In order to satisfy these basic objectives, the following tasks must be accomplished:

a. Seismic systems that possess relatively high magnifications in the pass band from 30 to 100 seconds must be designed, fabricated, tested, and installed both on the surface and within the mine at Grand Saline.

b. The vaults containing the seismometers must be sealed to the extent that pressure variations with periods as great as 400 seconds are strongly attenuated within the vault.

c. A microbarograph array must be operated at the surface in close proximity to the seismometer vaults in order to determine the frequency wave number content of the atmospheric noise.

In the event that atmospherically-generated seismic noise does prove to contribute significantly to the surface seismic background within the pass band of interest, methods to reduce its effect must be developed and evaluated. At the present time, it appears that this contribution could be significantly reduced by either of the following methods.

a. Installation of the sensors at moderate depths;

b. Estimation of the atmospherically-generated component of the seismic noise using microbarograph array data. This estimation would then be used to eliminate the actual component by subtracting it from the observed field.

Both methods should be evaluated thoroughly. It is recommended that the estimation process be evaluated during the studies at Grand Saline since high quality microbarographic data will be available. The degree of attenuation with depth, however, cannot be studied at Grand Saline since it is difficult, if not impossible, to move the seismic system vertically within the mine. A more effective technique for evaluating this method would be to operate a long-period triaxial seismograph system at various depths within a borehole and compare the results with observations taken at the surface. More specific recommendations regarding a study that will employ borehole observations to study the attenuation of atmospherically-generated noise with depth will be made at a later date pending the outcome of the studies at Grand Saline.

9. REFERENCES

Capon, J., 1969, Investigations of long-period noise at the Large Aperture Seismic Array: Jour. Geophys. Res., v. 74, p. 3182-3194

Der, Z. A., 1969, Long-period seismic noise and atmospheric pressure variations. Part 2. The response of a layered half space to atmospheric pressure changes: Geotech, A Teledyne Company, Technical Note 4/69 (in publication).

Rodgers, P. N., 1968, The Response of the horizontal pendulum seismometer to Rayleigh and Love waves, tilt, and free oscillations of the earth: Bull. Seis. Soc. Am., v. 58, p. 1385-1406

Sorrells, G. G., 1969, Long-period seismic noise and atmospheric pressure variations. Part 1. The response of an isotropic half space to a plane pressure wave: Geotech, A Teledyne Company, Technical Note 3/69 (in publication)

Von Seggern, D. H., 1969, A long-period noise study at Murphy Dome, Alaska: Seismic Data Laboratory Report No. 247.

APPENDIX 1 to TECHNICAL REPORT NO. 70-12

THE RESPONSE OF AN ISOTROPIC HALF-SPACE TO A PLANE PRESSURE WAVE

by

G. G. Sorrells

BLANK PAGE

THE RESPONSE OF AN ISOTROPIC HALF SPACE TO A PLANE PRESSURE WAVE

1. INTRODUCTION

A recent article by Capon, 1968, has suggested that seismic noise created by local variations in the atmospheric load may contribute significantly to the long-period noise field at periods greater than 20 seconds. This note is the first in a series of short papers describing the results of theoretical and experimental investigations of this hypothesis. This particular report is devoted to an analysis of the response of a perfectly elastic, isotropic half space to a plane pressure wave which moves at a constant rate well below the seismic wave speeds of the medium. This is a relatively simple problem which can be solved without resorting to numerical techniques. It has been considered by various authors (cf, Cole and Heath, 1958; Papadoulas, 1963; Ang, 1960; Payton, 1967). Our purpose in re-examining the solution is to determine if the earth's response to small changes in atmospheric pressure is sufficiently sensitive to warrant the study of more sophisticated models.

2. THEORY

Let x and z denote cartesian coordinates in directions parallel and normal to the surface of a half space. Let the plane z = 0 coincide with the surface of the half space and take z positive into the medium and x positive to the right of an arbitrarily chosen origin on the surface. Let α and β denote the compressional and shear wave velocities of the medium and let ρ denote the density. Suppose that a pressure disturbance p (x,t) is imposed upon the surface of the half space. Then letting $\sigma_{zz}(x,z,t)$ and σ_{zx} (x,z,t) denote the normal and tangential stresses, the boundary conditions are

$$\sigma_{zz}\ (x,\ 0,\ t) = p\ (x,\ t)\ = \frac{1}{4\pi^2} \iint_{-\infty}^{\infty} P\ (k,\ \omega)\ e^{i\omega t}\ e^{-ikx}\ dkd\omega \qquad (1)$$

$$\sigma_{zx}\ (x,\ 0,\ t) = 0 \qquad (2)$$

Now define displacement potentials ϕ and Ψ by

$$\phi\ (x,\ z,\ t) = \frac{1}{4\pi^2} \iint_{-\infty}^{\infty} A\ (\omega,k)\ e^{i\omega t}\ e^{-kx}\ e^{-\gamma z}\ dkd\omega \qquad (3)$$

$$\Psi(x,z,t) = \frac{1}{4\pi^2} \int_{-\infty}^{\infty}\int_{-\infty}^{\infty} B(\omega,k)\, e^{i\omega t}\, e^{-ikx}\, e^{-\gamma z}\, dk\,d\omega \tag{4}$$

where A and B are functions to be determined by the boundary conditions. It may be readily verified that these potentials satisfy the wave equations

$$\nabla^2\phi = \frac{1}{\alpha^2}\,\frac{\partial^2 \phi}{\partial t^2} \tag{5}$$

$$\nabla^2 \Psi = \frac{1}{\beta^2}\,\frac{\partial^2 \phi}{\partial t^2} \tag{6}$$

provided that

$$\gamma^2 = k^2 - k_\alpha^2 \tag{7}$$

$$\gamma^2 = k^2 - k_\beta^2 \tag{8}$$

where

$$k_\alpha^2 = \frac{\omega^2}{\alpha^2} \tag{9}$$

$$k_\beta^2 = \frac{\omega^2}{\beta^2} \tag{10}$$

In terms of the displacement potentials the normal and tangential stresses become (Ewing et al, 1957, p. 26)

$$\sigma_{zz}(x,z,t) = \lambda\,\nabla^2\,\phi + 2\mu\left(\frac{\partial^2 \phi}{\partial z^2} + \frac{\partial^2 \Psi}{\partial x \partial z}\right) \tag{11}$$

$$\sigma_{zx}(x,z,t) = \mu\left(2\,\frac{\partial^2 \phi}{\partial x \partial z} + \frac{\partial^2 \Psi}{\partial x^2} - \frac{\partial^2 \Psi}{\partial z^2}\right) \tag{12}$$

where

$$\lambda = \rho\ (\alpha^2 - 2\ \beta^2) \tag{13}$$

$$\mu = \rho\ \beta^2 \tag{14}$$

Then using the boundary conditions defined by equations 1 and 2 in equations 11 and 12 together with the definitions given by 3 and 4 the following relations for A and B are obtained

$$A\ (\omega,k) = \frac{(2k^2 - k_\beta^2)\ P\ (\omega,k)}{\mu\ F(\omega,k)} \tag{15}$$

$$B\ (\omega,k) = \frac{2i\ k\ \gamma\ \ P(\omega,k)}{\mu\ F\ (\omega,k)} \tag{16}$$

where

$$F(\omega,k) = (2k^2 - k_\beta^2)^2 - 4k^2\ \gamma\gamma' \tag{17}$$

Now let U(x,z,t), W(x,z,t) denote the displacements in the half space in the x and z directions, respectively. In terms of the potentials

$$U = \frac{\partial \phi}{\partial x} - \frac{\partial \psi}{\partial z} \tag{18}$$

$$W = \frac{\partial \phi}{\partial z} + \frac{\partial \psi}{\partial x} \tag{19}$$

and using equations 15 and 16 to replace A and B in equations 3 and 4 and then performing the operations described by equations 18 and 19, the following expressions for U and W are obtained

$$U(x,z,t) = \frac{-i}{4\pi^2} \int_{-\infty}^{\infty} \int_{-\infty}^{\infty} \frac{P\ (k,\omega)\ k\ [(2k^2 - k_\beta^2)e^{-\gamma z} - 2\gamma\gamma' e^{-\gamma' z}]}{F(k,\omega)} \tag{20}$$

$$e^{i\omega t}\ e^{-ikx}\ dk d\omega$$

$$W(x,z,t) = -\frac{1}{4\Pi^2\mu}\int_{-\infty}^{\infty}\int_{-\infty}^{\infty}\frac{P\ (k,\omega)\ \gamma\ [(2k^2-k_\beta{}^2)e^{-\gamma z}-2\ k^2e^{-\gamma' z}]}{F(k,\omega)} \qquad (21)$$

$$e^{i\omega t}e^{-ikx}\ dk\,d\omega$$

2.1 RESPONSE TO A PLANE WAVE SOURCE

The remainder of this note will be devoted to a study of the half space response to plane wave sources. A plane wave source is defined by the relation

$$p\ (x,t) = p\ (t - \frac{x}{c}) \qquad (22)$$

where c is the speed of the plane wave and, for the purposes of this study, is restricted to values such that $c << \beta$. Now

$$P(k,\omega) = \int_{-\infty}^{\infty}\int_{-\infty}^{\infty} p(x,t)\ e^{-i\omega t}\ e^{ikx}\ dt\ dx \qquad (23)$$

Therefore in the case of the plane wave source

$$P(k,\omega) = \int_{-\infty}^{\infty}\int_{-\infty}^{\infty} p(t-\frac{x}{c})\ e^{-i\omega t}\ e^{ikx}\ dt\ dx \qquad (24)$$

Let $\xi = t - \frac{x}{c}$

$$P(k,\omega) = \int_{-\infty}^{\infty} e^{i\ (k-\frac{\omega}{c})\ x}\ \int_{-\infty}^{\infty} P\ (\xi)\ e^{-i\omega\xi}d\xi\ dx \qquad (25)$$

$$= 2\pi P(\omega)\ \delta\ (k-\frac{\omega}{c}) \qquad (26)$$

Substitution of equation 26 into equations 20 and 21 and integration over k yields

$$U(x,z,t) = \frac{-i}{2\Pi_\mu} \int_{-\infty}^{\infty} \frac{P(\omega)\ \frac{\omega}{c}\ [(2\ \frac{\omega^2}{c^2} - \frac{\omega^2}{\beta^2})e^{-\gamma(\omega)z} - 2\gamma(\omega)\gamma'(\omega)e^{-\gamma'(\omega)z}]}{F\ (\frac{\omega}{c}, \omega)} \tag{27}$$

$$e^{i\omega(t-\frac{x}{c})}\ d\omega$$

$$W(x,z,t) = \frac{-i}{2\Pi\mu} \int_{-\infty}^{\infty} \frac{P(\omega)\gamma\ (\omega)\ [(2\ \frac{\omega^2}{c^2} - \frac{\omega^2}{\beta^2})\ e^{-\gamma(\omega)z} - 2\frac{\omega^2}{c^2}\ e^{-\gamma'(\omega)z}}{F\ (\frac{\omega}{c}, \omega)} \tag{28}$$

$$e^{i\omega(t-\frac{x}{c})}\ d\omega$$

where

$$\gamma\ (\omega) = \frac{|\omega|}{c}(1 - \frac{c^2}{\alpha^2})^{1/2} \tag{29}$$

$$\gamma'(\omega) = \frac{|\omega|}{c}(1 - \frac{c^2}{\beta^2})^{1/2} \tag{30}$$

Using the absolute value of ω assures that the displacements vanish as $z \to \infty$. Now for the case where $c << \beta$ we may write

$$\gamma\ (\omega) \approx \frac{|\omega|}{c}\ (1 - \frac{1}{2}\ \frac{c^2}{\alpha^2}) + O(\frac{c^4}{\alpha^4}) \tag{31}$$

$$\gamma'\ (\omega) \approx \frac{|\omega|}{c}\ (1 - \frac{1}{2}\ \frac{c^2}{\beta^2}) + O(\frac{c^4}{\beta^4}) \tag{32}$$

Therefore

$$e^{-\gamma z} \approx e^{-\frac{|\omega|}{c} z} \; e^{\frac{1}{2} \frac{|\omega|}{c} \frac{c^2}{\alpha^2}}$$

$$\approx e^{-\frac{|\omega|}{c} z} \left(1 + \frac{1}{2} \frac{\omega}{c} z \frac{c^2}{\alpha^2} + 0 \left(\frac{c^4}{\alpha^4}\right)\right) \tag{33}$$

$$e^{-\gamma' z} \approx e^{-\frac{|\omega|}{c} z} \left(1 + \frac{1}{2} \frac{|\omega|}{c} z \frac{c^2}{\beta^2} + 0 \left(\frac{c^4}{\beta^4}\right)\right) \tag{34}$$

and to the same order

$$\gamma(\omega)\gamma'(\omega) = \frac{\omega^2}{c^2} \left[1 - \frac{1}{2} \left(\frac{c^2}{\alpha^2} + \frac{c^2}{\beta^2}\right)\right] + 0 \left(\frac{c4}{\beta^4}\right) \tag{35}$$

Consequently part of equation (27) can be approximated

$$\frac{\omega}{c} \left[\left(2 \frac{\omega^2}{2} - \frac{\omega^2}{\beta^2}\right) e^{-\gamma(\omega) z} - 2\gamma(\omega) e^{-\gamma'(\omega) z} \right]$$

$$\approx \frac{\omega^3}{2} e^{-\frac{|\omega|}{c} z} \left[\left(2 - \frac{c^2}{\beta^2}\right) \left(1 + \frac{1}{2} \frac{|\omega|}{c} z \frac{c^2}{\alpha^2}\right)\right. \tag{36}$$

$$\left. -2 \left(1 - \frac{1}{2} \left(\frac{c^2}{\alpha^2} + \frac{c^2}{\beta^2}\right)\right)\right] \left(1 + \frac{1}{2} \frac{|\omega|}{c} z \frac{c^2}{\beta^2}\right)$$

$$\approx \frac{\omega^3}{c^2} e^{-\frac{|\omega|}{c} z} \left[\frac{|\omega|}{c} z \left(\frac{c^2}{\alpha^2} - \frac{c^2}{\beta^2} + \frac{c^2}{\alpha^2}\right) \right.$$

$$\approx \frac{\beta^2-\alpha^2}{\alpha^2\beta^2}\ \frac{\omega^3}{c}\ [\frac{\beta^2}{\beta^2-\alpha^2} + \frac{|\omega|}{c}\ ]e^{-\frac{|\omega|}{c}z} \qquad \text{(36 cont'd)}$$

Similarly part of equation (28) can be approximated

$$\gamma(\omega)\ [(2\frac{\omega^2}{c^2} - \frac{\omega^2}{\beta^2})\ e^{-\gamma(\omega)z} - 2\frac{\omega^2}{c^2}\ e^{-\gamma'(\omega)z}\ ]$$

$$\approx \frac{|\omega|^3}{c} e^{-\frac{\omega}{c}z}\ (1 - \frac{1}{2}\ \frac{c^2}{\alpha^2})\ [\frac{|\omega|}{c}\ z\ (\frac{c^2}{\alpha^2} - \frac{c^2}{\beta^2}) - \frac{c^2}{\beta^2}\ ] \qquad (37)$$

$$\approx \frac{\beta^2-\alpha^2}{\alpha^2\beta^2}\frac{|\omega|^3}{c}\ (\frac{\alpha^2}{\alpha^2-\beta^2} + \frac{|\omega|z}{c})\ e^{-\frac{|\omega|}{c}z}$$

and $$F(\frac{\omega}{c},\omega) \approx \frac{\omega^4}{c^4}\ [(2-\frac{c^2}{\beta^2})^2 - 4\ (1 - \frac{1}{2}\ \frac{c^2}{\alpha^2})(1 - \frac{1}{2}\ \frac{c^2}{\beta^2})\ ]$$

$$\approx \frac{\omega^4}{c^4}\ [4 - 4\frac{c^2}{\beta^2} - 4\ (1 - \frac{1}{2}\ (\frac{c^2}{\alpha^2} + \frac{c^2}{\beta^2})\ )\ ] \qquad (38)$$

$$\approx 2\ \frac{\omega^4}{c^2}\ [\frac{\beta^2-\alpha^2}{\alpha^2\beta^2}\ ] \qquad (39)$$

Now

$$\frac{\beta^2}{\beta^2-\alpha^2} = -\frac{\mu}{\lambda+\mu} \tag{40}$$

$$\frac{\alpha^2}{\alpha^2-\beta^2} = \frac{\lambda+2\mu}{\lambda+\mu} \tag{41}$$

Using equations 36 through 41 in 27 and 28, one obtains for U and W

$$U(x,z,t) = \frac{ic}{4\pi\mu} \int_{-\infty}^{\infty} P(\omega) \frac{\left(\frac{\mu}{\lambda+\mu} - \frac{|\omega|}{c} z\right) e^{-\frac{\omega}{c} z} e^{i\omega\left(t-\frac{x}{c}\right)}}{|\omega|} d\omega \tag{42}$$

$$W(x,z,t) = -\frac{c}{4\pi\mu} \int_{-\infty}^{\infty} P(\omega) \frac{\left(\frac{\lambda+2\mu}{\lambda+\mu} + \frac{|\omega| z}{c}\right) e^{-\frac{\omega}{c} z} e^{i\omega\left(t-\frac{x}{c}\right)}}{|\omega|} d\omega \tag{43}$$

Equations 42 and 43 describe a seismic disturbance which propagates at the same rate as the imposed pressure field. It may be readily verified that this disturbance is identical in form to that created by a static load p (x) imposed upon the surface of the half space (cf, Sneddon, 1951). Furthermore it is important to note that in this particular case there is no energy transport by the normal seismic waves (i.e., waves traveling at speeds α or β or the Rayleigh wave velocity). To an observer moving at the same speed as the load, the disturbance would remain fixed and would be identical to that created by a static load.

2.2 DISCUSSION

The basic question to be answered in this technical note is whether or not the seismic disturbance created by the pressure wave can contribute significantly to the seismic background. In order to answer this question, the vertical and horizontal displacements created by a sinusoid of angular frequency ω_o traveling at a speed c_o meters/sec with a pressure amplitude of P microbars are determined below for various half-space models. For this case

$$P(\omega) = P \int_{-\infty}^{\infty} e^{i(\omega-\omega_o)t}\, dt \tag{44}$$

$$= 2\Pi\ P\ \delta\ (\omega-\omega_o)$$

Using equation 44 in equations 42 and 43 and performing the indicated integration, the displacement components are found to be

$$U(x,z,t) = \frac{ic_o P\left(\frac{\mu}{\lambda+\mu} - \frac{|\omega_o|}{c_o} z\right) e^{-\frac{\omega_o}{c_o} z}\ e^{i\omega_o\,(t-\frac{x}{c_o})}}{2\mu\ |\omega|} \tag{45}$$

$$W(x,z,t) - \frac{c_o P\ \left(\frac{\lambda+2\mu}{\lambda+\mu} + \frac{|\omega_o|}{c_o} z\right) e^{-\frac{|\omega_o|}{c_o} z}\ e^{i\omega_o\,(t-\frac{x}{c_o})}}{2\mu\ |\omega_o|} \tag{46}$$

Now at the surface the displacements become

$$U(x,o,t) = \frac{ic_o P}{2(\lambda+\mu)}\ \frac{e^{\ i\omega_o\ (t\ -\ \frac{x}{c_o})}}{\omega_o} \tag{47}$$

$$W(x,o,t) = \frac{c_o P}{2\mu} - \frac{(\lambda+2\mu)}{(\lambda+\mu)}\ \frac{e^{i\omega_o\ (t\ -\ \frac{x}{c_o})}}{\omega_o} \tag{48}$$

Equations 47 and 48 have been used to compute the amplitudes of the displacement components for various models with $c_o = 5, \frac{\Pi}{10} \leq \omega_o \leq \frac{\Pi}{50}$ ($20 \leq T \leq 100$ sec) and P = 1. The models are described in table 1. The results are displayed in figures 1 through 4 for both the vertical and horizontal components of displacement.

Table 1. Parameters of the models used to compute vertical and horizontal components of displacement

Model No.	α km/sec	β km/sec	ρ g/cm^3	Geology
1	0.3	0.1	1.6	Unconsolidated sediments
2a	2.9	0.7	2.3	Sedimentary rock
2b	2.9	1.0	2.3	Sedimentary rock
3	4.8	2.8	2.65	Sedimentary rock
4	5.8	3.25	2.85	Granites

Model 1 is clearly an extreme case and was included to show the worst possible conditions. As shown in figure 1 this model is quite sensitive to small changes in atmospheric pressure. For instance, in the period range 20-40 seconds, the average vertical displacement is 80 mμ for a pressure amplitude of 1 μ bar. In the same range the average horizontal displacement is 10 mμ/μ bar. These results imply that one of the reasons that long-period installations located on thick sections of alluvial fill are generally characterized by high noise levels is that the unit is quite sensitive to small changes in atmospheric pressure.

Models 2a-2b have velocities and densities characteristic of many sandstone shale sequences found in the mid-continent and Gulf Coast regions of the United States. Model 2b differs from 2a only in that the shear wave velocity has been increased to 1 km/sec. The curves shown in figure 2 indicate that the pressure sensitivity of these models is considerably lower than the unconsolidated sediments model.

In the period range 20-40 seconds the average vertical displacement is about 1 mμ/μ bar for Model 2a and 0.6 mμ/μ bar for Model 2b. However, if we assume pressure amplitudes on the order of 100 μ bars, the corresponding vertical displacements of the surface would be 100 and 60 mμ for Models 2a and 2b. Now, in general, the vertical seismic background observed at periods greater than 25 seconds is somewhere on the order of 100-200 mμ. Thus, the pressure waves with amplitudes of 100 μ bars or more can generate a significant fraction of the seismic background at periods greater than 25 seconds. If the installations

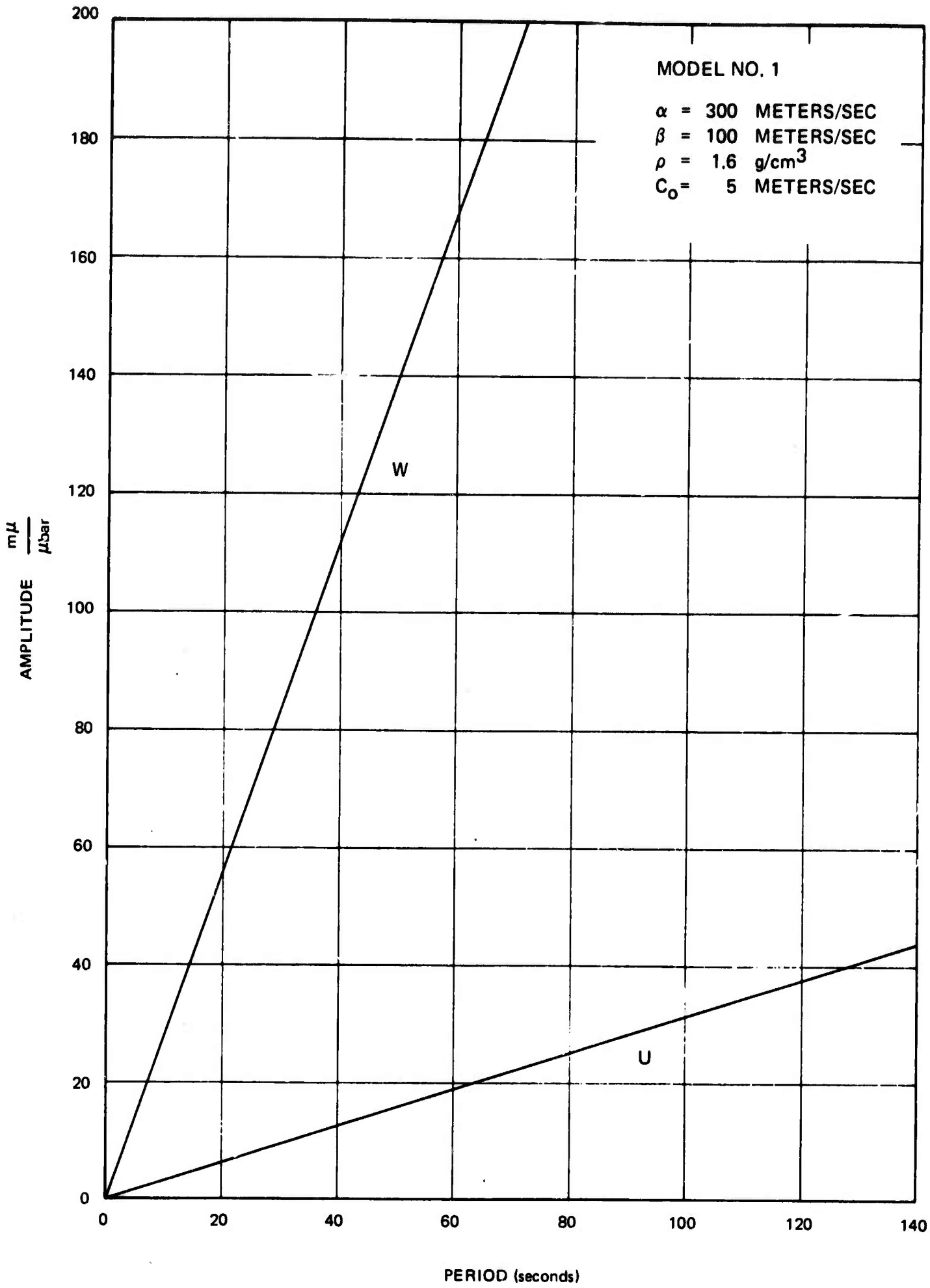

Figure 1. Surface displacement response of a half space consisting of unconsolidated sediments

G 5828

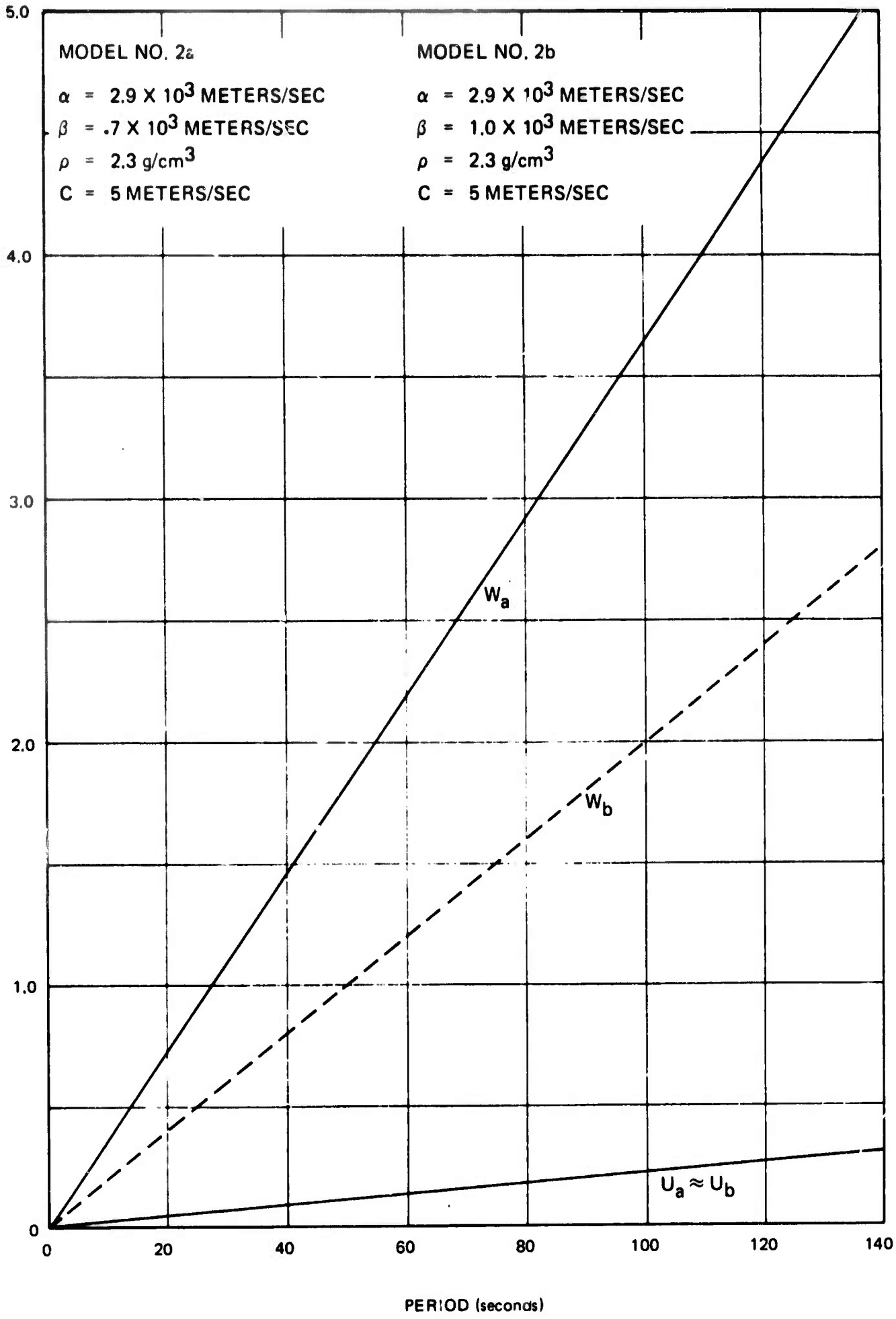

Figure 2. Surface displacement response of a weak sandstone shale half space

G 5829

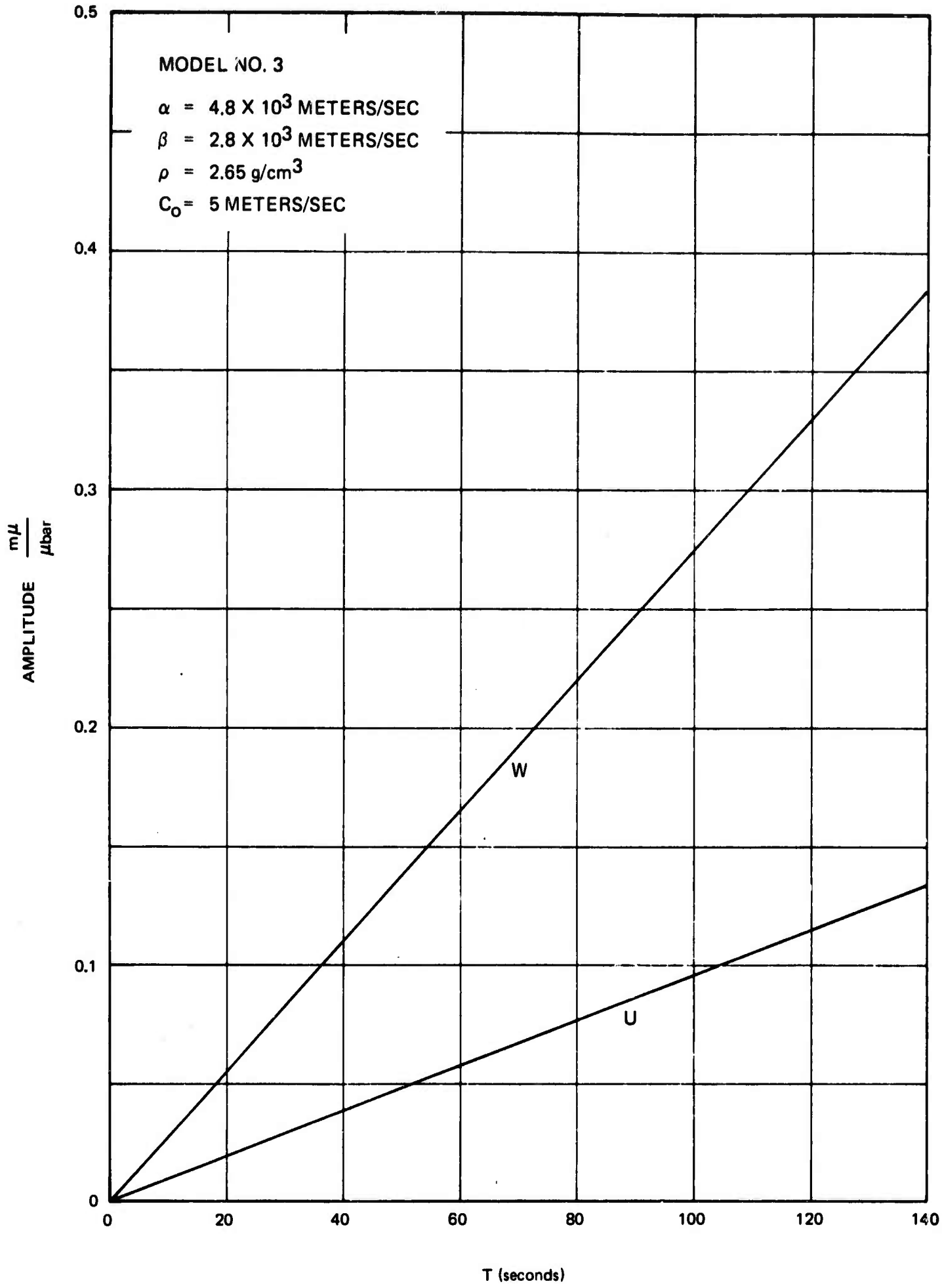

Figure 3. Surface displacement response for a competent sedimentary rock half space

G 5830

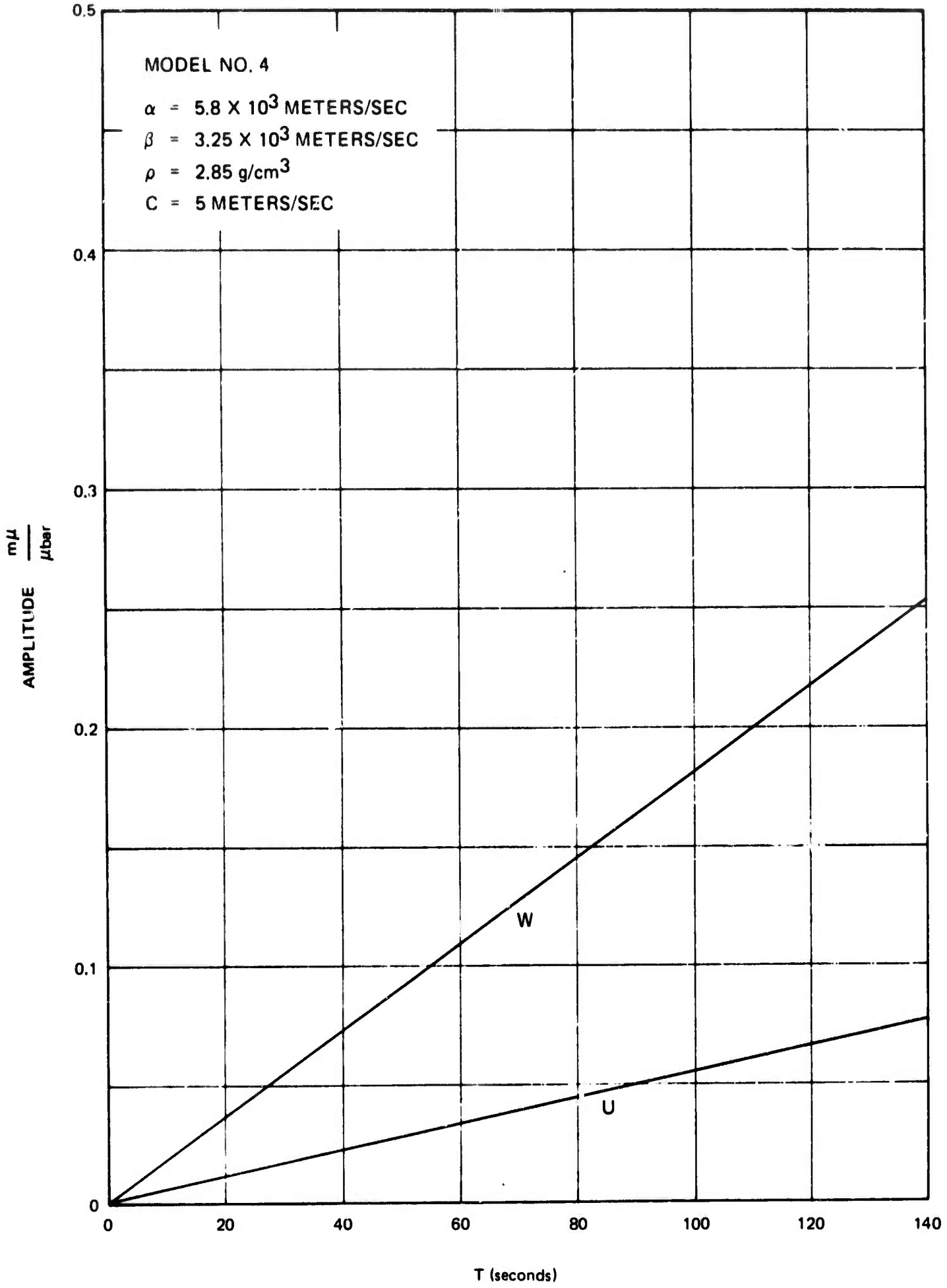

Figure 4. Surface displacement response for a granite half space

G 5831

happen to be located on a thick section of moderately to poorly indurated sandstones and shales. By thick it is meant that the dimensions of section are much larger than the wavelength of the disturbance. For the periods and speeds considered above the corresponding wavelengths would be less than 200 meters. Consequently, these results could be applied to sections whose dimensions are as small as a kilometer. It is important to note that the shallow structure beneath the Montana LASA is quite similar to that used in Model 2b at least down to depths of about 1.5 km (cf, Glover and Alexander, 1968). Thus, it appears reasonable to expect that, at the Montana LASA, atmospherically-generated seismic noise can contribute significantly to the vertical long-period noise spectrum as suggested by Capon (1968).

The situation is quite different for the more competent rocks which are represented by Models 3 and 4. As shown in figures 3 and 4, the sensitivity of these models to atmospheric pressure fluctuations has been reduced by about an order of magnitude relative to the sandstone-shale models considered previously. Therefore, in rocks of this type, displacements caused by atmospheric loading cannot contribute significantly to the long-period seismic noise background unless the pressure amplitudes are on the order of a millibar or more.

The previous paragraphs have been concerned with the displacements at the surface of the earth caused by a plane pressure wave. These waves also produce tilts, which can be a major source of noise on the long-period horizontal seismograph system. The tilts produced by a plane pressure wave may be determined in the following way.

Let Θ (x, z, t) be the angle of tilt measured from the horizontal. Then

$$\text{Tan } \Theta \text{ (x, z, t)} = \frac{dW}{dx}$$

or using equation 46

$$\text{Tan } \Theta \text{ (x,z,t)} = \frac{iP}{2\mu} \left[\left(\frac{\lambda+2\mu}{\lambda+\mu}\right) + \frac{\omega_o}{c_o} z\right] e^{-\frac{\omega_o}{c_o} z} e^{i\omega_o \left(t - \frac{x}{c_o}\right)} \qquad (49)$$

Since Θ is generally small

$$\text{Tan } \Theta \approx \Theta$$

Consequently at z = 0

$$\Theta \approx \text{Tan } \Theta = \frac{P}{2\mu} \frac{\lambda+2}{(\lambda+\mu)} e^{i \left[\omega_o \left(t - \frac{x}{c_o}\right) + \frac{\pi}{2}\right]} \qquad (50)$$

Thus, at the surface the amplitude of the tilt is dependent only upon the elastic constants of the medium and the pressure amplitude and is independent of frequency. The tilts associated with a 1 microbar pressure amplitude in each of the four models described above are listed in table 2.

Table 2. Tilts caused by a plane pressure wave with a 1 μ bar amplitude

Model No.	Tilt (radians)
1	3.5×10^{-9}
2a	4.6×10^{-11}
3	3.5×10^{-12}
4	2.2×10^{-12}

It can be seen from this table the tilts at the surface are quite small. However, because of the tilt sensitivity of the long-period horizontal seismometer, even these small tilts can produce large apparent horizontal dis-displacements. Rogers (1968) has shown that the apparent horizontal displacements caused by tilt is given by

$$U_\Theta = \Theta \frac{gT^2}{4\Pi^2} G(T) \qquad (51)$$

where T is the period

G (T) is the displacement response of the horizontal seismograph system

g is the local value of gravity

U_Θ is the apparent trace displacement caused by tilt

U_Θ was computed using the values of Θ listed in table 2, a pressure amplitude of 100 microbars, and the standard LRSM long-period displacement response for $20 \leq T \leq 100$ seconds. The resulting values are for a system operating at a magnification of 10^4 at 25 seconds and are plotted as a function of period in figure 5. The curves in this figure indicate that during periods of moderate atmospheric turbulence systems located in thick sections of unconsolidated sediments will become virtually unusuable. The situation is not much better for the case of Model 2. In a thick sandstone shale sequence, the tilts would generate trace displacements between about 40 and 90 mm, if the system were operating at magnification of 10^4.

In the more competent rocks a pressure amplitude of 100 microbars would generate trace amplitudes varying from 2-7 mm of trace displacement at a magnification of 10^4. Thus, it would appear that the combination of moderate atmospheric turbulence and the tilt sensitivity of the long-period horizontal seismometer can limit the magnifications possible at the surface to about 1 to 2 x 10^4 even for the more competent rocks. This is in qualitative agreement with our experience that long-period horizontal seismograph systems can rarely be operated at magnifications exceeding 2 x 10^4 at or near the surface of the earth.

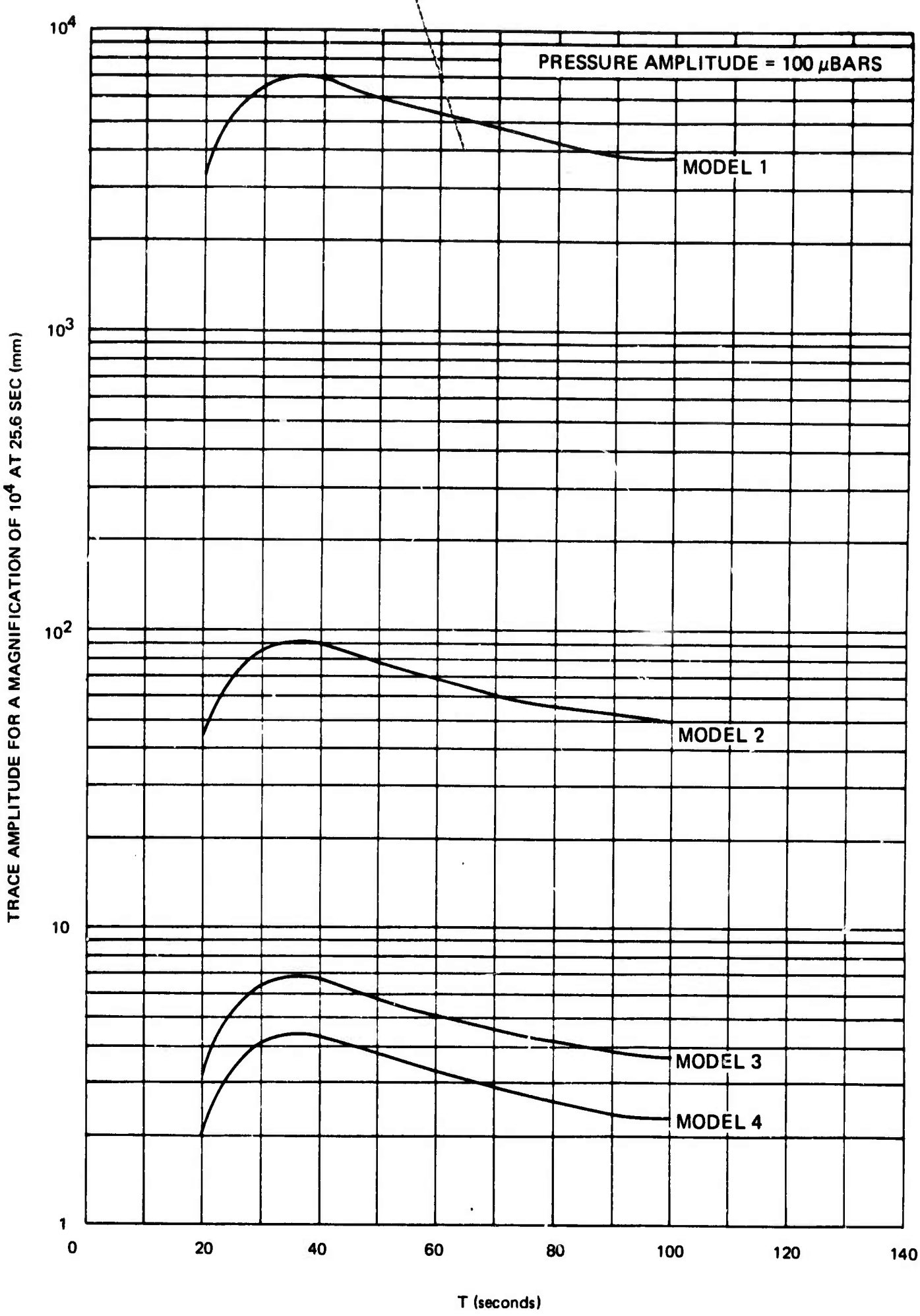

Figure 5. Trace displacements on a horizontal long-period seismograph with a standard LRSM response caused by earth tilts

G 5832

2.3 ATTENUATION WITH DEPTH

An interesting feature of the half-space response to slowly moving plane pressure waves is the rate at which the disturbance decays away with depth. Let $R_w(z)$ denote the ratio of the vertical displacement at depth to the vertical displacement at the surface. Then from equations 46 and 48

$$R_w(z) = \frac{\left(\frac{\lambda+2\mu}{\lambda+\mu} + \frac{\omega_o}{c_o} z\right)}{\frac{\lambda+2\mu}{\lambda+\mu}} e^{-\frac{\omega_o}{c_o} z} \qquad (52)$$

Similarly, if $R_u(z)$ denotes the ratio of the horizontal displacement at depth z to the horizontal displacement at the surface, then from equations 45 and 47

$$R_U(z) = \frac{\frac{\mu}{\lambda+\mu} + \frac{\omega_o z}{c_o}}{\frac{\mu}{\lambda+\mu}} e^{-\frac{\omega_o}{c_o} z} \qquad (53)$$

If we let $R_\Theta(z)$ define a similar ratio for the tilts it is clear from equations 48 and 50 that

$$R_\Theta(z) = R_N(z) \qquad (54)$$

$R_w(z)$ is plotted as a function of z in figure 6 for the cases where $c = 5$ $\lambda + 2\mu/\lambda + \mu = 1.0$ and 1.5, and for periods 20, 40, and 60 seconds. Generally, the results show that the attenuation with depth is weakly dependent on the elastic properties of the medium. The values 1.0 and 1.5 span the practical range of values that the ratio $\lambda + 2\mu/\lambda + \mu$ can assume for rocks, with the higher values being associated with the more competent rocks. It can be seen from the curves in this figure that the differences in attenuation with depth between poorly consolidated and competent rocks is only 2 dB.

Furthermore, the seismic disturbance will decay rapidly with increasing depth. For example, at a depth of 100 meters (328 ft), the amplitude of a 20-second period sinusoid would be 40 dB below the amplitude observed at the surface. At the same depth, waves with periods of 40 and 60 seconds would be reduced by about 11 and 6 dB, respectively. However, in order to obtain a 40 dB reduction of the noise generated by atmospheric pressure variations over the period range from 20 to 60 seconds, the detectors would have to be placed at least 300 meters deep.

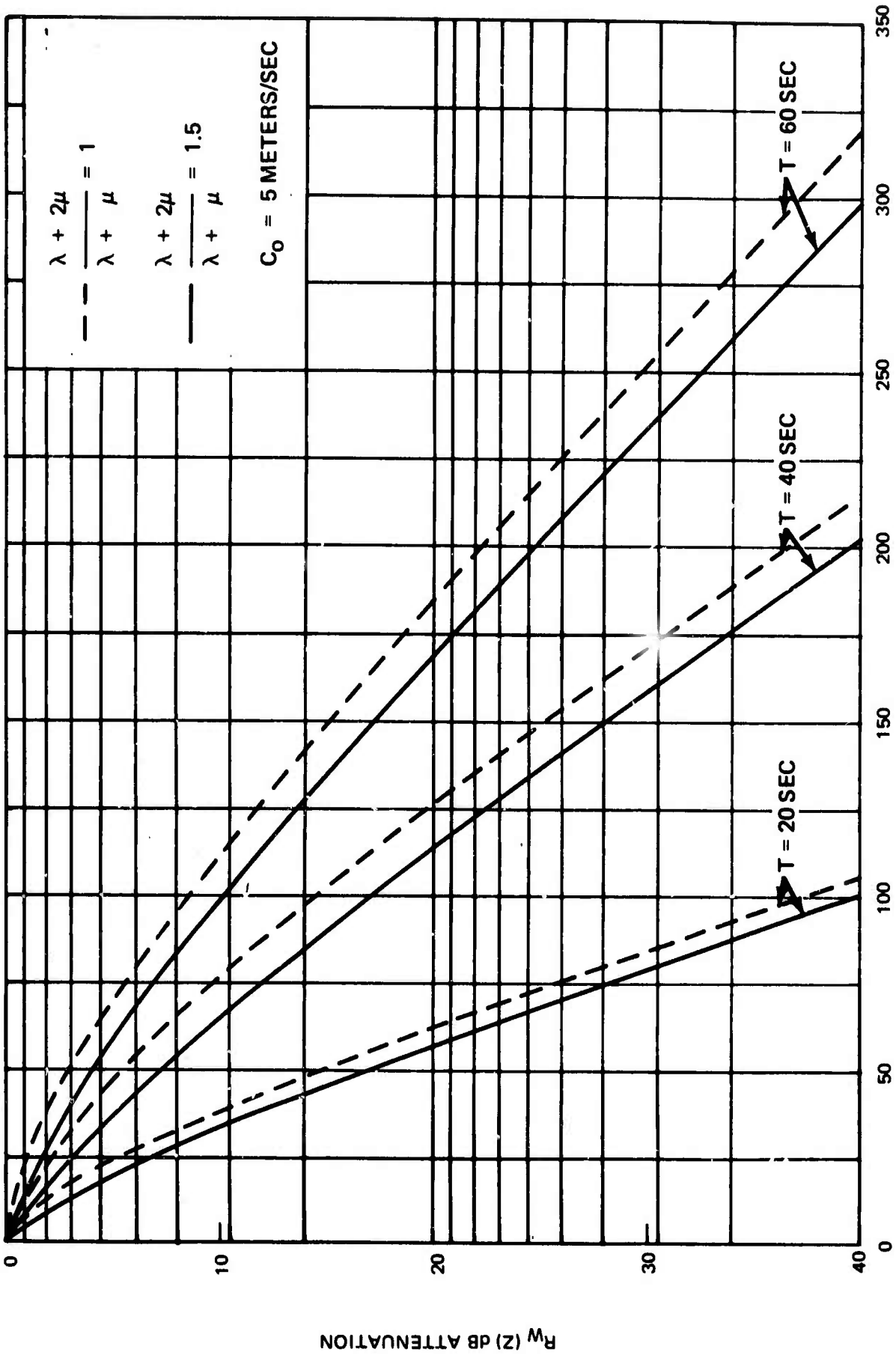

G 5833

Figure 6. Attenuation of vertical displacements and tilts with depth

These results suggest that in regions where local atmospherically-generated seismic noise can be anticipated to be significant at the surface (i. e., in regions of thick sandstone-shale sequences or alluvial fill) much of this type of noise can be eliminated by placing the detector at moderately shallow depths.

One further point requires emphasis. Recently, there has been a considerable interest in extending the response of long-period systems to cover a pass band from 30 to 100 seconds. From equations 47 and 48 it is seen that the displacement response of the half space increases linearly with increasing period. Furthermore, equation 51 shows that the tilt response of the horizontal seismograph system will increase as the square of the period. Consequently, on the basis of these results, one can anticipate that atmospherically generated seismic noise will place severe restrictions on the magnifications that can be obtained with ultra long-period systems which are operated near the surface.

3. CONCLUSIONS

The basic purpose of this initial study was to determine if the displacements and tilts generated by plane pressure waves can contribute significantly to the long-period noise field. On the basis of the results presented in the previous paragraphs, it appears that the vertical displacements generated by these waves can contribute significantly to the long-period noise field provided that

a. The installation is located at or near the surface of a section of alluvial fill or poorly to moderately indurated sandstones and shales which is at least 1 km thick, and

b. The pressure amplitudes are of the order of 100 microbars or greater.

Pressure waves with amplitudes of the order of 100 microbars will also create significant tilt noise on long-period horizontal seismograph systems located at or near the surface, regardless of the rock type. However, the noise will be much less severe on competent units.

The results also show that the seismic disturbances created by plane pressure waves will decay rapidly with depth. Furthermore, the rate of decay is virtually independent of the rock type. The implications are that the contribution of atmospherically-generated noise to the long-period background can be virtually eliminated for periods less than a minute by placing the detectors at depths on the order of 300 meters.

Finally, it appears that atmospherically generated noise will be more severe on ultra long-period systems than on presently operating systems.

These results are considered to be sufficiently significant to warrant the study of the response of more complex media to more realistic pressure fields. Consequently, numerical techniques to compute the response of layered media to arbitrary pressure fields are being developed.

4. BIBLIOGRAPHY

Ang, D. D., 1960, Transient motion of a line load on the surface of an elastic half space; Q. App. Math., vol. 18, p. 251-256

Capon, J., 1968, Investigation of long-period noise at LASA: Lincoln Laboratories Tech. Rept. 1968-15, 60 p.

Cole, J. D., and J. H. Heath, 1958, Stresses produced in a half plane by moving loads: Jour. Applied Mech., vol. 25, p. 433-436

Ewing, W. M., W. S. Jardetzky, and F. Press, 1957, Elastic waves in layered media: McGraw-Hill Book Co., New York, 380 p.

Glover, P., and S. S. Alexander, 1968, Lateral variations in crustal structure beneath the Montana LASA, Seismic Data Laboratory Rept. No. 205, 20 p.

Papadopoulos, M., 1963, The elastodynamics of moving loads: Part 1, the field of a semi-infinite line load moving on the surface of an elastic solid with constant supersonic velocity: Jour. Austral. Math. Soc., vol. 3, p. 79-92

Payton, R. G., 1967, Transient motion of an elastic half space due to a moving surface line load; Int. Jour. Engineering Sci., vol. 5, p. 49-79

Rodgers, P. W., 1968, The response of the horizontal pendulum seismometer to Rayleigh and Love waves, tilt, and free oscillations of the earth: Bull. Seis. Soc. Am., vol. 58, no. 5, p. 1385-1406

Sneddon, I. N., 1951, Fourier Transforms: McGraw-Hill Co., New York, 542 p.

APPENDIX 2 to TECHNICAL REPORT NO. 70-12

STATIC LOADING OF A LAYERED ELASTIC HALF SPACE BY ATMOSPHERIC PRESSURE VARIATIONS

by

Zoltan A. Der

STATIC LOADING OF A LAYERED ELASTIC HALF SPACE BY ATMOSPHERIC PRESSURE VARIATIONS

1. INTRODUCTION

The response of a homogeneous elastic half space to moving loads has been discussed in Appendix 1 (Sorrells). This appendix shows how to compute the response of a layered elastic half space to static loads. The Haskell-Thompson matrix method is used to derive displacements and tilts for the two dimensional case. It is likely that the layered half space is a more satisfactory model in actual field situations, and the computer programs will be used to verify the theory in conjunction with field experiments.

2. GENERAL

Suppose that the stresses at the free surface of a layered elastic solid (the earth) due to atmospheric pressure variations can be described as space-time stationary random processes with power spectral densities $P_{3i}(\omega, k_1, k_2)$ where ω is the angular frequency and k_1 and k_2 are the horizontal wave numbers and i = 1, 2, 3 indices for the three coordinate axes. It is assumed that the coordinate axes x_1 and x_2 are horizontal and x_3 is pointing downward into the elastic half space. If the velocities of the pressure variation are considerably below the elastic velocities in the elastic half space, the deformations of the half space can be considered as static and the dependence of the response on ω can be neglected. Therefore, the response of the elastic half space will depend, in the first approximation, only on the horizontal wave numbers k_1 and k_2. Both shear and normal stresses can act on the surface. Shear stresses are usually due to wind drag and pressure on irregularities and obstacles at the surface, such as trees, hills, buildings, etc. In the following discussion it will be assumed that the earth's surface is flat, and the seismometers are located far from obstacles which would cause wind drag. For a flat earth the normal stresses $P_{33}(\omega, k_1, k_2)$ would cause the tilts observed. In order to derive the pressure variations observed by a microbarograph it is assumed that the components of the pressure field with different k_1 and k_2 are independent and therefore the power spectra of these pressures are additive. This is not an unreasonable assumption and therefore power spectra of the microbarograph output can be obtained by integration over k_1 and k_2 giving

$$P_{mm}(\omega) = M^2(\omega) \int_{-\infty}^{\infty}\int P_{33}(\omega,k_1,k_2)dk_1dk_2 \qquad (1)$$

where $M(\omega)$ is the frequency response of the microbarograph. A horizontal seismograph oriented in a direction x_j located at a certain depth d_1 below the surface would record the tilt with the power spectra (using the same logic)

$$_jP_{ss}(\omega) = S^2(\omega) \int_{-\infty}^{\infty}\int T_j{}^2(k_1,k_2,d_1)P_{33}(\omega,k_1,k_2)dk_1dk_2 \qquad (2)$$

Where $S(\omega)$ is the seismometer tilt response function and $T_j(k_1,k_2,d_1)$ is the static tilt response of the ground at depth d_1 to normal loads of the form exp i $(k_1x_1+k_2x_2)$ acting at the surface. The cross spectra between the microbarograph and horizontal seismometer or two horizontal seismometers located at depths d_1 and d_2 and similarly oriented will be

$$_iP_{sm}(\omega) = M(\omega)S(\omega) \int_{-\infty}^{\infty}\int T_j(k_1,k_2,d_1)\ P_{33}(\omega,k_1,k_2)\,dk_1dk_2 \qquad (3)$$

$$_jP_{s_1s_2}(\omega) = S_1(\omega)S_2(\omega) \int_{-\infty}^{\infty}\int T_j(k_1,k_2,d_1)T_j(k_1,k_2,d_2)P_{33}(\omega,k_1,k_2)dk_1dk_2$$

where $S_1(\omega)$ and $S_2(\omega)$ are the responses of seismometers. Similar expressions can be written for the response of the vertical seismometers, but since these instruments are sensitive to vertical displacements and not to tilts, the effect of atmospheric loading would be much smaller on these instruments. It can be shown from the above expression that even if the noise from other sources is absent, and the atmospheric noise is propagating unidirectionally, the coherence between the outputs of the microbarograph and a seismometer, or between two seismometers located at two different depths is always less the unity unless $T_j(k_1,k_2,x_3) \equiv$ const. The tilt response is constant for a homogeneous halfspace at $x_3=0$ for the two-dimensional case where one of the horizontal wavenumbers is zero. If such model of the subsurface and unidirectional propagating noise is applicable, the coherence between the seismometer tilt output and the microbarograph may be close to unity. In other cases it is necessary to know more about the f-k structure of the atmospheric pressure variations.

In order to determine the f-k structure of the atmospheric pressure variations microbarograph array measurements are necessary. If such measurements are available the above theory can be verified from simultaneous pressure and tilt recordings. $T_j(k_1,k_2,x_3)$ can be determined numerically if the elastic parameters of the subsurface are known. It is assumed here that the subsurface can be modeled with a layered elastic half space, and the effect of the vault cavity at depth can be neglected.

The purpose of this study is to develop methods to eliminate tilt noise caused by atmospheric pressure variations on horizontal long-period seismometers. If the f-k structure of the pressure variations is such that a reasonable number of microbarographs is sufficient to predict the tilt noise on the seismometers, a significant reduction of the noise on long-period seismographs is possible. A single microbarograph is not likely to achieve this goal, since the f-k field depends on the wind direction and even if a halfspace model and two-dimensional pressure field are applicable the sign of the phase lag of $\pi/2$ between the pressure variations and the tilt, and the magnitude of tilt in direction x_j must be determined from the horizontal pressure gradient. To estimate this gradient an array of at least three microbarographs is necessary. The knowledge of wind direction and speed may reduce the number of microbarographs necessary.

If the average f-k structure of the atmospheric pressure variations is known at a certain location one can estimate the number of microbarographs and seismometers needed to eliminate a certain fraction β of loading noise power by computing the multiple coherence functions $\gamma(\omega)$, defined by (Bendat and Piersol, 1966) as

$$\gamma^2(\omega) = 1 - [G_i(\omega)G^i(\omega)]^{-1},$$

for various combinations of sensors, where $G_i(\omega)$ and $G^i(\omega)$ are the i-th diagonal elements of the spectral matrix and inverse spectral matrix of sensor outputs. The elements of these matrices can be computed for any layered structure and instrument combination by using formulas of the type (1), (2), and (3). The sensor combination which yields $\gamma_i(\omega) \geq \beta$ would be sufficient to eliminate this fraction of loading noise power at the i-th sensor.

The mathematics used in computation of tilt responses is described in appendices 2a and b. The computer programs are described in appendix 2c.

APPENDIX 2a to TECHNICAL REPORT NO. 70-12

PROPAGATION MATRIX FOR TWO-DIMENSIONAL DEFORMATION OF A LAYERED ELASTIC HALF SPACE DUE TO SURFACE LINE STRESSES

PROPAGATION MATRIX FOR TWO-DIMENSIONAL DEFORMATION OF A LAYERED ELASTIC HALF SPACE DUE TO SURFACE LINE STRESSES

This theory is based on the extension of results described by Sneddon (1951) for two-dimensional deformation of elastic solids, the Fourier transform G of the Airy stress function with respect to the horizontal coordinate x_1 is satisfied by the equation

$$\left(\frac{d^2}{dx_3} - k^2\right)^2 G = 0 \tag{1}$$

where k is the horizontal wave number, x_3 is the vertical coordinate. This equation has the general solution

$$G = (A + Bx_3)e^{-|k|x_3} + (C + Dx_3)e^{|k|x_3} \tag{2}$$

The Fourier transforms of the stresses and displacements can be derived from this equation the following way

$$u = \frac{1+\sigma}{E}\left[\frac{(\sigma - 1)}{k^2}\frac{d^3G}{dx_3^3} + (2-\sigma)\frac{dG}{dx_3}\right]$$

$$v = i\frac{1+\sigma}{E}\left[(1-\sigma)\frac{d^2G}{dx_3^2} + \sigma k^2 G\right]\frac{1}{k} \tag{3}$$

$$\tau_{33} = -k^2 G$$

$$\tau_{13} = ik\frac{dG}{dx_3}$$

where u, v, τ_{xx}, τ_{xy} are the vertical and horizontal displacements, normal and sheer stresses at the surface, respectively, σ is the Poisson ratio, E is the Young's modulus of the elastic medium.

For a layered medium consisting of homogenous isotropic layers the Solution (2) can be propagated by the Thompson-Haskell matrix method where A, B, C, and D take the place of constants Δ'_m, $\Delta''m$, $\omega'm$, $\Delta''m$ in Haskell's paper. The matrix which is equivalent of Haskell's D_m for this boundary value problem can be obtained by substituting 2 into 3. It takes the form,

$$D_m = \begin{vmatrix} \frac{1+\sigma_m}{E_m} & 0 & 0 & 0 \\ 0 & \frac{1+\sigma_m}{E_m} & 0 & 0 \\ 0 & 0 & 1 & 0 \\ 0 & 0 & 0 & 1 \end{vmatrix} \begin{vmatrix} k & 1+kd_m-2\sigma_m & -k & i-kd_m-2\sigma_m \\ -k & kd_m+2\sigma_m-2 & k & kd_m-2\sigma_m+2 \\ -k^2 & -k^2d_m & -k^2 & -k^2d_m \\ -k^2 & k(1-kd_m) & k^2 & k(1-kd_m) \end{vmatrix} \begin{vmatrix} e^{-kd_m} & 0 & 0 & 0 \\ 0 & e^{-kd_m} & 0 & 0 \\ 0 & 0 & e^{kd_m} & 0 \\ 0 & 0 & 0 & e^{kd_m} \end{vmatrix}$$

where d_m is the layer thickness, E_m and σ_m are the elastic constants E and σ for layer m.

In the halfspace below the layers C and D must vanish in order to have decreasing displacements and stresses with depth.

APPENDIX 2b to TECHNICAL REPORT NO. 70-12

INTEGRATION IN THE k_1 - k_2 PLANE

INTEGRATION IN THE k_1 - k_2 PLANE

The two-dimensional loading program can be used to compute the integrals of the type (1), (2), and (3) if the integration performed is a polar coordinate system. In this case $k_1 = k\cos\phi$, $k_2 = k\sin\phi$, $dk_1dk_2 = kdkd\phi$ $P(\omega,k_1,k_2) \sim P(\omega,k,\phi)$, $T_1(k_1,k_2,d) \sim T(k,d)\cos\phi$, etc.

Therefore, the power spectrum of the microbarograph will become

$$P_{mm}(\omega) = M^2(\omega) \int_{k=0}^{\infty} \int_{\phi=0}^{2\Pi} k\, P_{33}(\omega,k,\phi)\, d\phi dk$$

The tilt power spectrum on the seismometers oriented in the directions of horizontal coordinate axis x_1 and x_2, respectively, and located at depth d will become

$$P_{11}(\omega) = S_1(\omega) \int_{k=0}^{\infty} \int_{\phi=0}^{2\Pi} k\, P_{33}(\omega,k,\phi) T^2(k,d) \cos^2\phi\, d\phi dk$$

$$P_{22}(\omega) = S_2(\omega) \int_{k=0}^{\infty} \int_{\phi=0}^{2\Pi} k\, P_{33}(\omega,k,\phi)\, T^2(k,d) \sin^2\phi\, d\phi dk$$

where ϕ is measured from the x_1 axis

The cross spectrum between the microbarograph and the seismometer oriented in the x_1 direction will become

$$P_{m1}(\omega) = S_1(\omega)\, M(\omega) \int_{k=0}^{\infty} \int_{\phi=0}^{2\Pi} k\, P_{33}(\omega,k,\phi)\, T(k,d)\, |\cos\phi|\, d\phi dk$$

A number of similar formulas can be derived for other instrument combinations.

APPENDIX 2c to TECHNICAL REPORT NO. 70-12

GENERAL DESCRIPTION OF COMPUTER PROGRAM LOAD 2

BLANK PAGE

GENERAL DESCRIPTION OF COMPUTER PROGRAM LOAD 2

A computer program LOAD 2 has been written for the calculation of the displacements and tilts. The program computes the responses of the layered medium to sinusoidal stresses at the surface as functions of wavelength and depth. Both normal and shear stresses can be applied. The program reads the densities, the stresses and seismic velocities of the layers, the ranges of horizontal wave numbers at the surface. It is a simple matter to use the program to compute the deformation of the layered medium due to stresses of arbitrary shape by Fourier synthesis of sinusoidal loads. The same program can be used to compute strains due to surface stresses at any depth, and with some modifications, to compute stresses and displacements due to dislocations of certain types in a layered medium.

Some numerical problems can arise if the displacements are computed for greater depths using large wave numbers; after reading the value near zero at a certain depth the displacements start to increase without bound with increasing depth. The problem is purely numerical and is similar in nature to that encountered in surface wave calculations (Dunkin 1965). It can be remedied by double precision calculations or the elimination of the large (and obviously erroneous) displacement values below a certain depth.

The matrix alegebra is analogous to that presented by Haskell (1953), products like $D_m E_m^{-1}$ are computed numerically by inverting E_m and multiplying instead of deriving all the algebra.

The program has been checked out against formulas derived by Sorrells (1969) and several other examples in the literature.

Figures 1 to 6 show some examples of calculations performed using the formulas presented above.

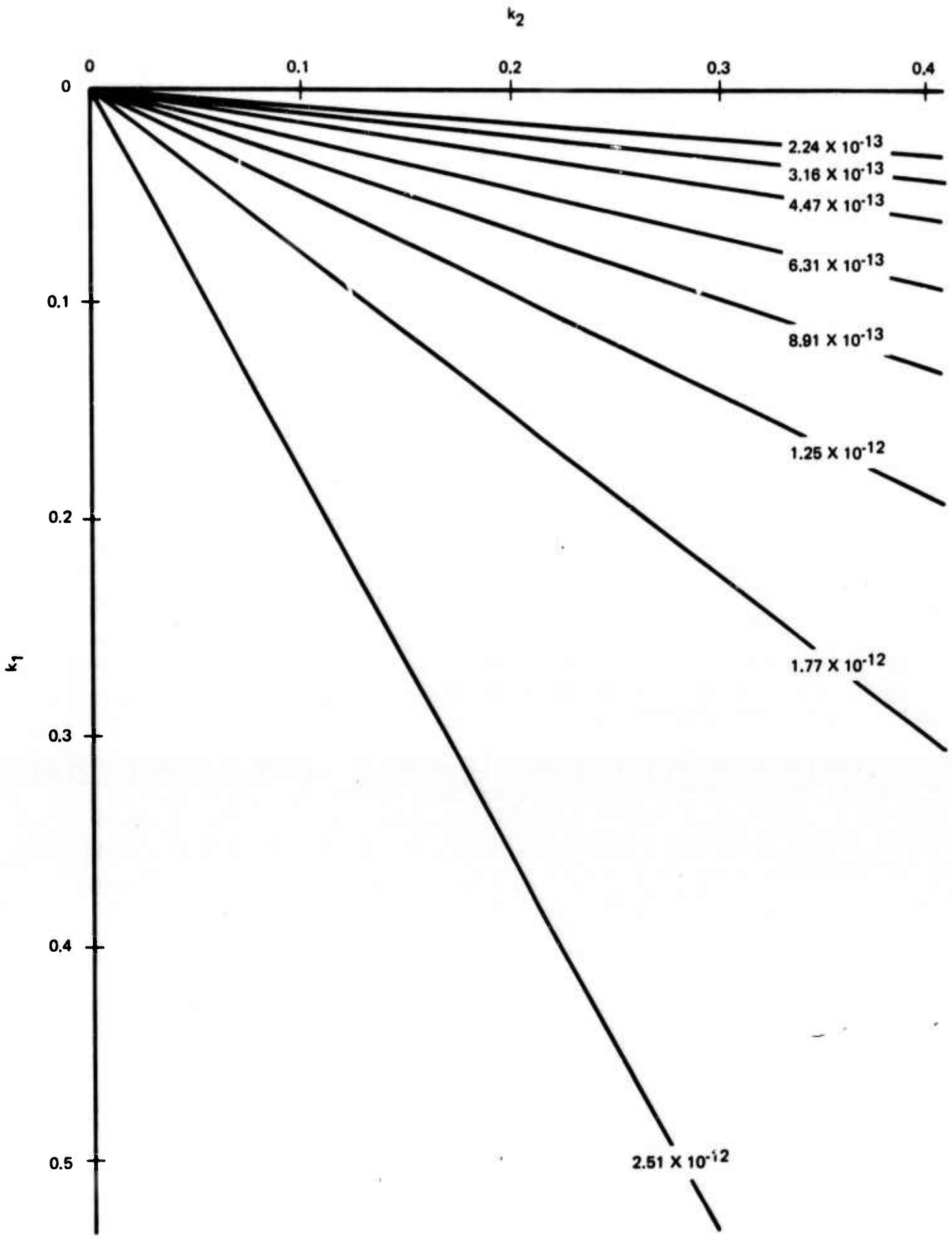

Figure 1. Half-space, surface

G 5834

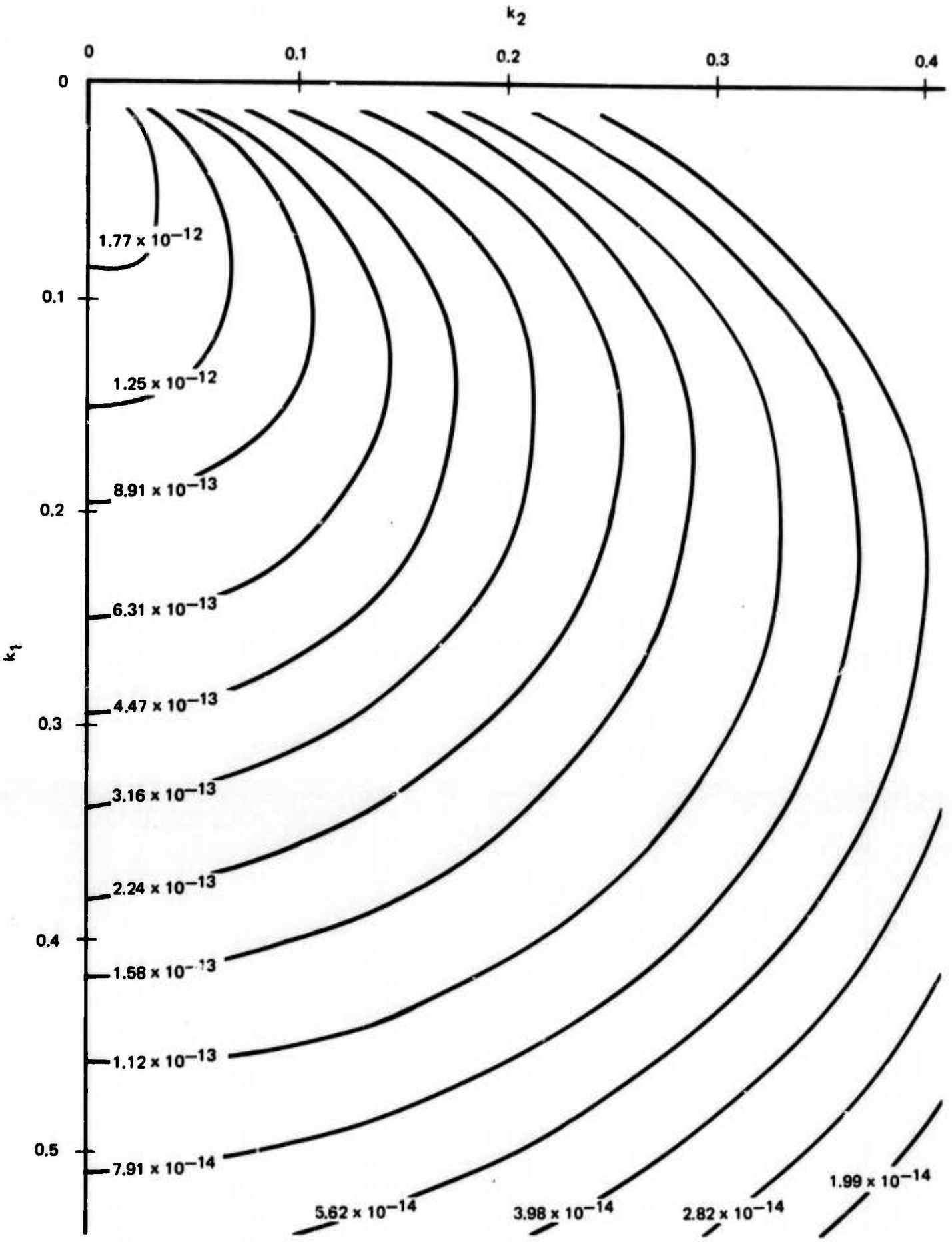

Figure 2. Half-space, depth of 10 meters

G 5835

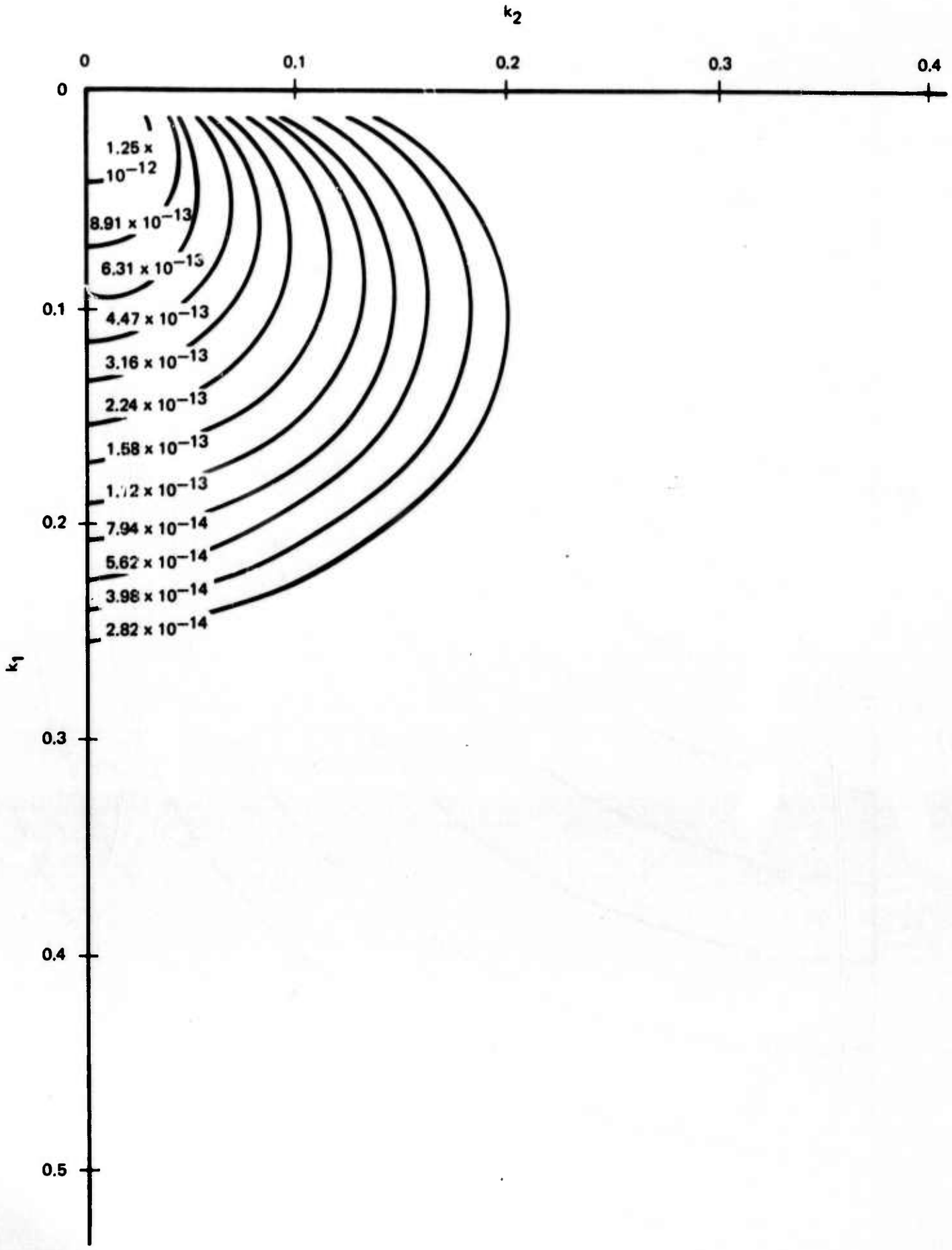

Figure 3. Half-space, depth of 25 meters

G 5836

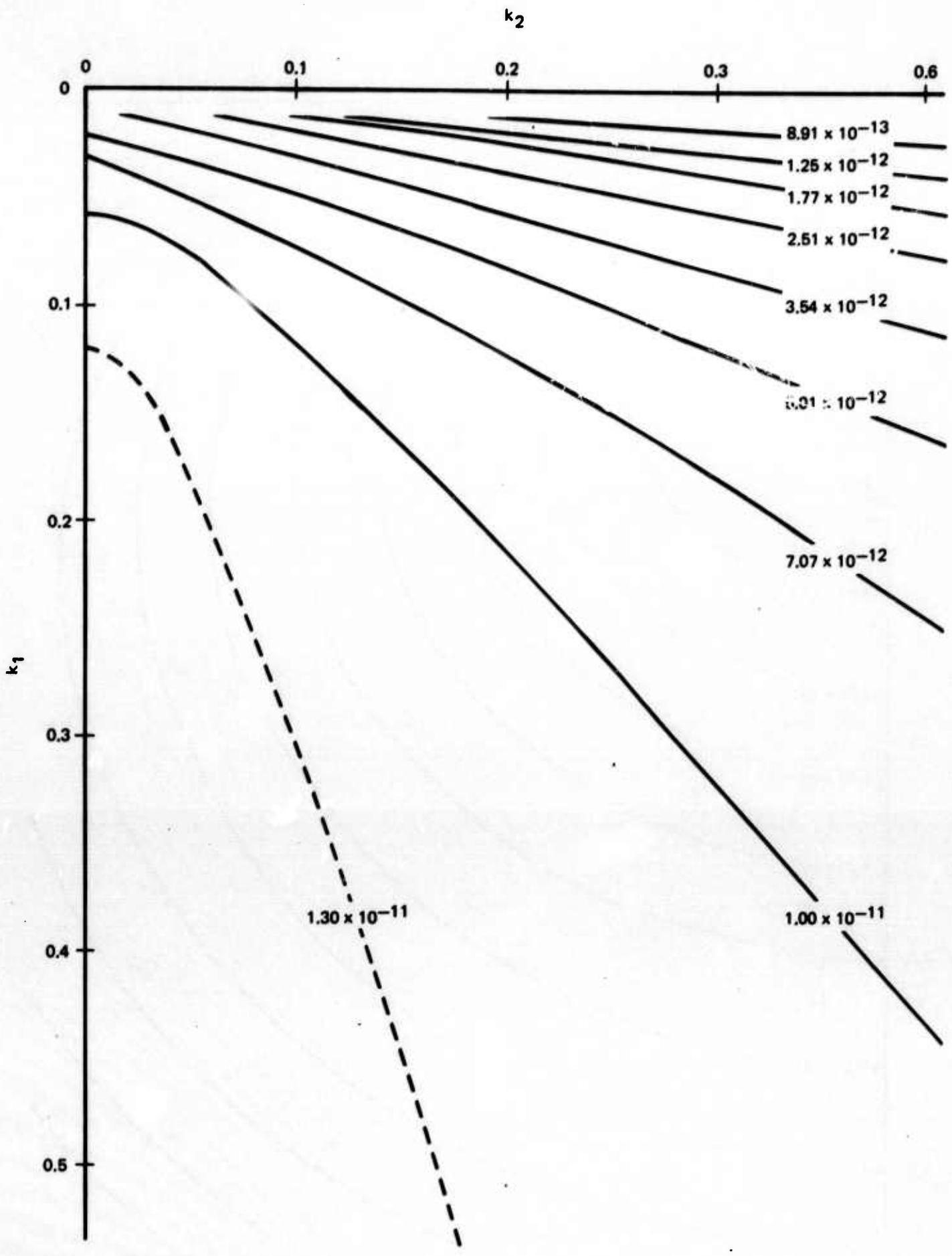

Figure 4. Low velocity layer-surface

G 5837

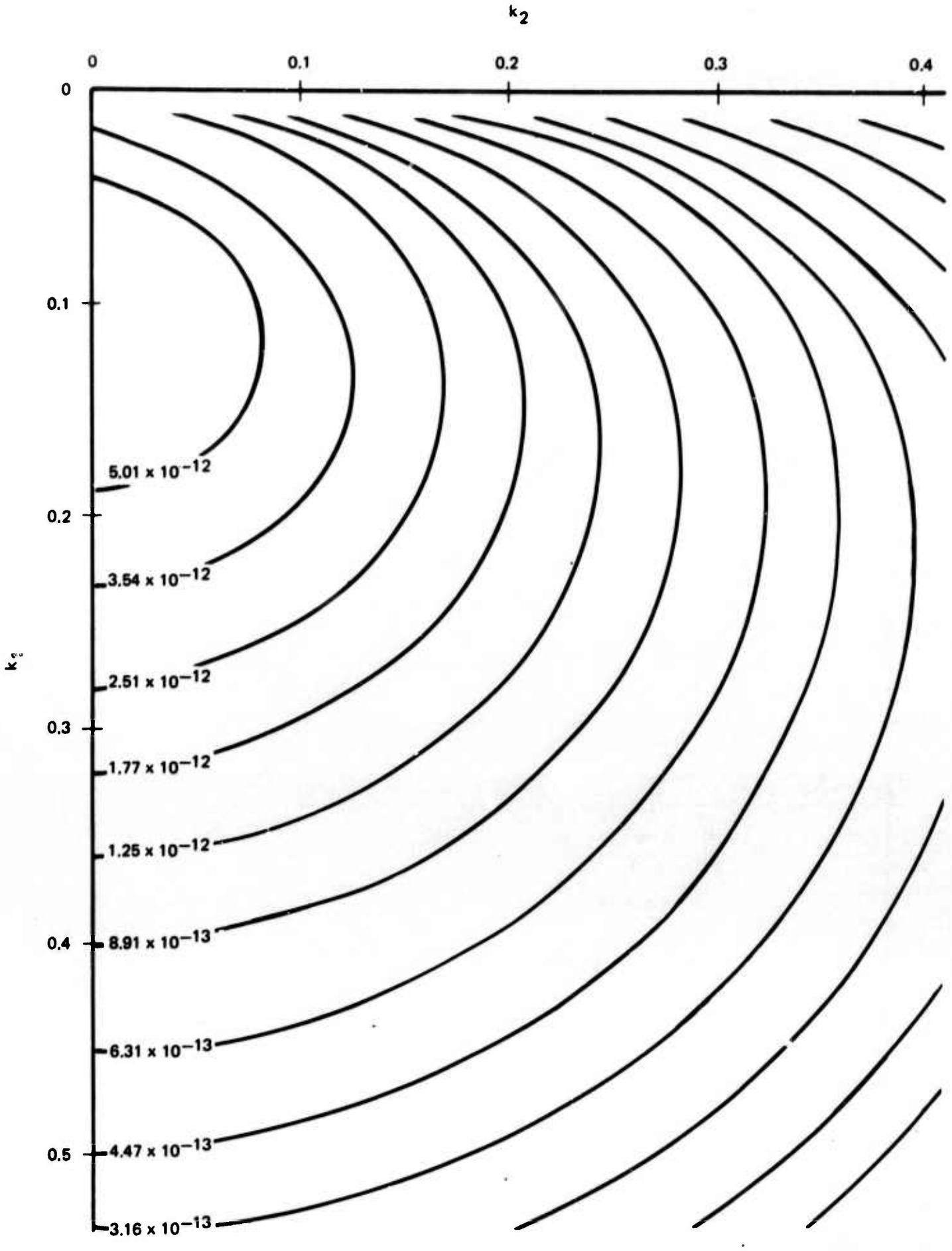

Figure 5. Low velocity layer-depth 10 meters

G 5838

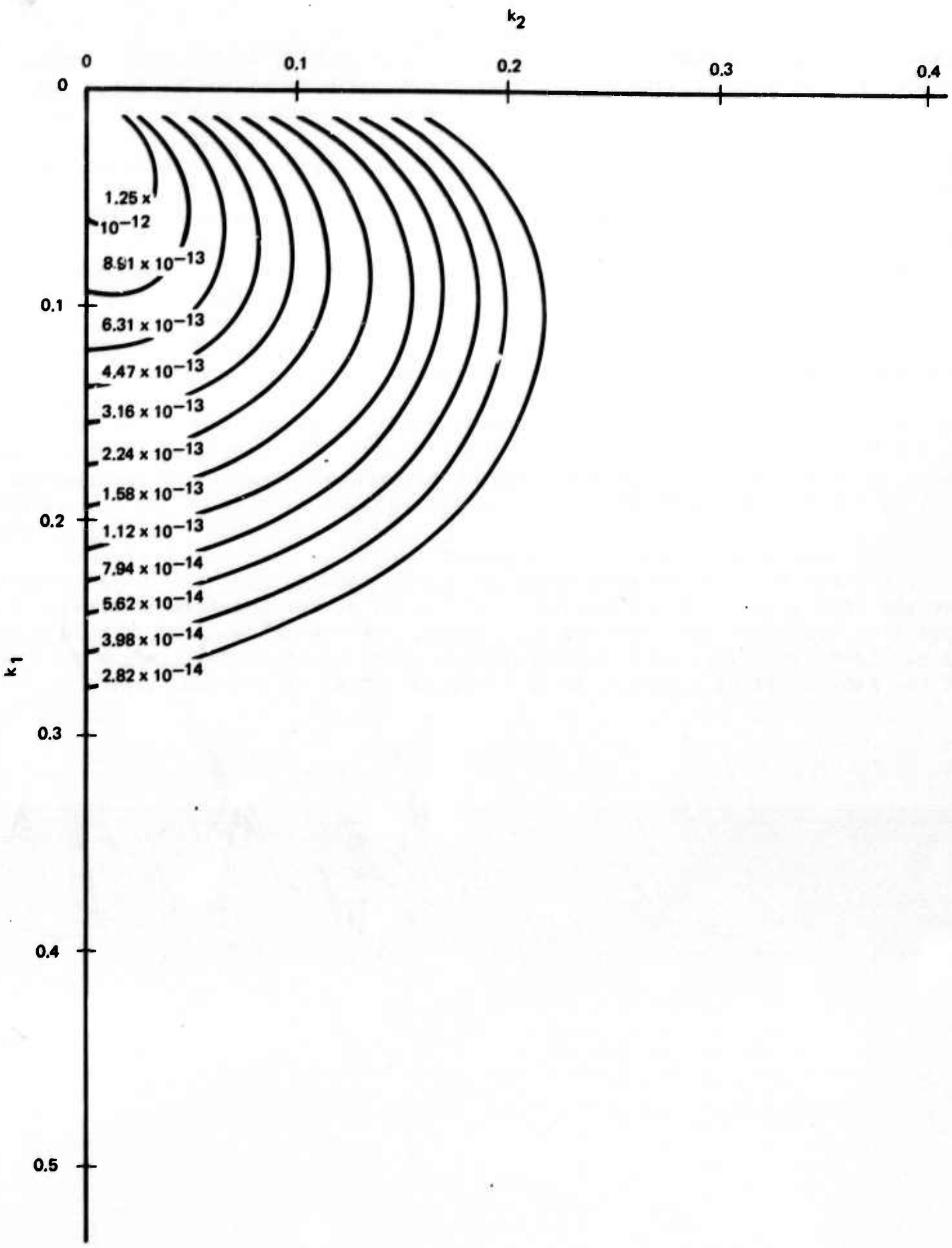

Figure 6. Low velocity layer-depth 25 meters

G 5839

Figures 1 to 3 show contour plots of the tilt responses in the x_1 direction T_1 (k_1, k_2, d) as functions of horizontal wave numbers k_1 and k_2 for a surface load of form exp i (k_1 x 1 + k_2 x 2) with 1 μbar amplitude. The model used is a halfspace with compressional and shear velocities of 5.5 and 3.3 km/sec, respectively, and density 2.5 g/cm^3. The k_1-k_2 response is contoured for three different depths; 0 (surface), 10 and 25 m. The contours are drawn at 3 dB intervals and the tilt is given in radians. The contours were done by hand over sparse network of numerical values and therefore are not very accurate, but the figures are given only as illustrations of the general nature of the responses. On the k_2 axis the response has to be zero. The figures show the fast decay of the short wavelengths with depth. Figures 4 to 6 show the tilt responses for a model with a low velocity layer overlying a half space with elastic constants given above.

The velocities and density for the low velocity layer are the following; V_p = 3 km/sec, V_s = 1.6 km/sec and δ = 2. g/cm^3. The thickness of the layer is 25 m. At the surface for large wave numbers the response resembles that of a half space with elastic constants equalling those of the low-velocity layer.

At 25 m depth the tilt is very small and it is almost equal to the tilt response for the half space. This indicates that burial of seismometers is a very effective technique for reducing tilt noise. If the seismometer is buried close to the lower interface of a surface low-velocity layer the tilt noise is about at the same level as it would be in competent rocks at the same depth.

REFERENCES

Bendat, J. S., and A. G. Piersol (1966)
Measurement and analysis of random data, John Wiley and Sons, New York, p. 230-231

Dunkin, J. W. (1965)
Computation of modal solutions in layered, elastic media at high frequencies, Bull. Seismol. Soc. Am. 55, p. 335-358

Haskell, N. A. (1953)
The dispersion of surface waves on multilayered media: Bull. Seismol. Soc. Am. 43, p. 17-43

Sneddon, I. N. (1951)
Fourier transforms: McGraw-Hill, New York, p. 402-406

Sorrells, G. G. (1969)
Long-period seismic noise and atmospheric pressure variations, Part 1. Geotech, Science Services Technical Memorandum #4.

UNCLASSIFIED

Security Classification

DOCUMENT CONTROL DATA - R & D

(Security classification of title, body of abstract and indexing annotation must be entered when the overall report is classified)

1 ORIGINATING ACTIVITY (Corporate author)

Teledyne Geotech
Garland, Texas 75040

2a. REPORT SECURITY CLASSIFICATION

Unclassified

2b. GROUP

3 REPORT TITLE

Long-Period Seismic Noise and Atmospheric Pressure Variations

4 DESCRIPTIVE NOTES (Type of report and inclusive dates)

Technical Report

5 AUTHOR(S) (First name, middle initial, last name)

G. G. Sorrells
Zoltan Der

6 REPORT DATE	7a. TOTAL NO. OF PAGES	7b. NO. OF REFS
	76	10

8a. CONTRACT OR GRANT NO.	9a. ORIGINATOR'S REPORT NUMBER(S)
F33657-69-C-0757	Technical Report No. 70-12
b. PROJECT NO. VELA T/8703	
c.	9b. OTHER REPORT NO(S) (Any other numbers that may be assigned this report) None
d.	

10 DISTRIBUTION STATEMENT

This document is subject to special export controls and each transmittal to foreign governments for foreign nationals may be made only with prior approval of Chief, AFTAC

11. SUPPLEMENTARY NOTES	12. SPONSORING MILITARY ACTIVITY
None	Air Force Technical Applications Center

13. ABSTRACT

Preliminary studies of the long-period seismic noise and the atmospheric pressure fields were made at the Kleer mine near Grand Saline, Texas, during the winter of 1968. The results of the studies indicate that during periods of atmospheric turbulence the vertical and horizontal components of the seismic noise field observed at the surface may increase in total power by as much as 16 and 34 dB within the period range from 20 to 60 seconds. In contrast, long-period systems operated in the mine show little change in power levels regardless of the atmospheric conditions at the surface. The observations are consistent with the hypothesis that the increase observed at the surface is caused by atmospherically-generated deformations of the earth. However, because of questions regarding the surface vaults capability to attenuate pressure changes, the possibility that the noise was caused by vault leakage must be considered an equally likely explanation at the present time. The results indicate that atmospherically-generated seismic noise can seriously degrade the capability of a long-period surface installation to detect surface waves. Because of this finding, further more definitive studies are recommended.

DD FORM 1 NOV 65 1473

UNCLASSIFIED

Security Classification

14 KEY WORDS	LINK A		LINK B		LINK C	
	ROLE	WT	ROLE	WT	ROLE	WT
Long-Range Seismic Measurements Program						
VELA-Uniform						
Seismic						
Detection of Seismic Signals						
Long-Period Seismic Noise						
Atmospheric Pressure Variations						
Static Loading						